NOISE AND VIBRATION PROBLEMS OF RECIPROCATING MACHINERY

by

LT. FRANKLIN F. ALVAREZ, U. S. N.

SUBMITTED IN PARTIAL FULFILLMENT OF THE REQUIREMENTS

FOR THE DEGREE OF NAVAL ENGINEER

and

FOR THE DEGREE OF MASTER OF SCIENCE
IN MECHANICAL ENGINEERING

at the

MASSACHUSETTS INSTITUTE OF TECHNOLOGY

May, 1964

THESIS SUPERVISOR: DONALD ROSS, PH. D.

NOISE AND VIBRATION PROBLEMS OF RECIPROCATING MACHINERY

by

LT. FRANKLIN F. ALVAREZ, U.S.N.
B.S., UNITED STATES NAVAL ACADEMY
(1957)

SUBMITTED IN PARTIAL FULFILLMENT
OF THE REQUIREMENTS FOR THE
DECREE OF NAVAL
ENGINEER
and
FOR THE DEGREE OF MASTER OF
SCIENCE IN MECHANICAL
ENGINEERING
at the
MASSACHUSETTS INSTITUTE OF
TECHNOLOGY
May, 1964.

Signature of Author -
Department of Naval Architecture and
Marine Engineering, May 22, 1964

Certified by -
Thesis Supervisor .

Certified by -
Thesis Adviser.

Accepted by -
Chairman, Departmental Committee
on Graduate Students.

ABSTRACT

Noise and Vibration Problems of Reciprocating Machinery
Lt. Franklin F. Alvarez, USN

Submitted to the Department of Naval Architecture and Marine Engineering on May 22, 1964 in partial fulfillment of the requirements for the degree of Naval Engineer and the Master of Science degree in Mechanical Engineering.

The objective of this thesis are to extend the analysis of piston slap as a noise source in reciprocating machines, to confirm experimentally the analysis of this source, and to study other impacts in order to better identify, understand, and predict the major noise sources in reciprocating machines. Analysis of the effects of wrist pin and crankshaft offset on piston slap as well as analysis of bearing slap and valve impacts are included.

Noise and vibration data are also included from a series of experiments with a single-cylinder diesel engine conducted with variations of piston clearance and speed while the engine was both fired and motored. Valve impact effects were also obtained.

It is found that negative offset reduces piston impacts and so does reduced piston clearances. Piston slap and combustion effects are dominant in the mid frequency range while valve noise dominates the high frequency range. Also the noise and vibration levels increase sharply with speed. Bearing slaps were not found to be important.

It is recommended that noise and vibration levels be reduced by designing reciprocating machines with negative offset, small piston clearances, slower speed operation, and ports instead of valves for two stroke operation.

Thesis Supervisor: Dr. Donald Ross.

ACKNOWLEDGEMENT

I wish to express my appreciation to Dr. Donald Ross who first made known to me the idea of piston slap. His help and guidance over the past year has enriched my knowledge and understanding of noise reduction problems.

I am also indebted to Dr. Ungar of Bolt Beranek and Newman who aided me with the piston slap theory, Prof. Den Hartog who gave me a broader understanding of mechanics, Bolt Beranek and Newman for furnishing the instrumentation, M.I.T.'s Experimental Projects Laboratory for furnishing the diesel engine and help in setting up the experiment, and the many others who helped me with this thesis.

TABLE OF CONTENTS

TABLE OF CONTENTS (CONT'D)

LIST OF FIGURES

LIST OF FIGURES (CONT'D)

LIST OF TABLES

I. INTRODUCTION

A. BACKGROUND

In recent years because of the growing importance of the submarine and of anti-submarine warfare, the Navy has become very interested in ship silencing techniques. In both submarines and surface ships reciprocating machinery such as diesel engines and compressors have been found to be among the noisiest. Not only do these machines help to provide detection for the enemy and interfere with their own ship's sonor, but also in some cases the airborne noise levels in engine rooms are so high as to be harmful to the operators. Thus there has been an emphasis on quieting reciprocating machinery and diesel engines in particular.

A number of studies (10, 13, 14, 15) have been conducted to determine the dominant sources in diesel engines for both the structure-borne, underwater radiated sound and the airborne sound. Intakes and exhausts have been found to be the dominant sources of airborne noise when they are not properly muffled, but there is no general agreement as to the major sources contributing to the structure-borne sound or the airborne sound on properly muffled engines. The two sources most often advocated are engine unbalance and combustion pressure pulses. However, an analysis of the vibrations induced by the engine unbalance and bending of the crankshaft (3, 8, 11, 17) shows lines at harmonics of engine rotational speed and does not account for the numerous lines of high frequency vibrations that contribute much of the radiated noise.

Likewise, the studies dealing with noise caused by combustion pressures (1, 2, 5, 7) do not adequately account for the middle and high frequency noise levels found in typical diesel engine spectra. Nor do they explain why the spectra shapes for diesels show almost no change even when load, injection timing, and quality of fuel are varied. Also, cylinder pressures

in compressors are not subject to combustion and yet these reciprocating machines have high noise levels and spectra similar to diesel engines. Thus there seems to be some other major noise source that is responsible for the high noise levels found in reciprocating machines.

B. PISTON SLAP

In the mid-1950's V.I. Zinchenko (20, 21) studied the effect of piston slap, i.e. the impact of the piston on the liner in a transverse direction, in numerous Russian diesel engines. He developed a noise parameter and showed that the diesels studied correlated well with this parameter. Other studies dealing with liner cavitation (6, 9, 12) confirmed the existence of piston slap and gave evidence of high energy high frequency vibrations being induced by this phenomenon. This then offers a possible explanation for the source of the high frequency vibrations and radiated noise associated with most reciprocating machines. Although an extension of Zinchenko's work on piston slap (19) has been completed, there is no evidence of experiments having been conducted in which the parameters which control piston slap were varied. Also, in addition to piston slap, other impacts such as the opening and closing of valves and bearing slap, which result from the reciprocating nature of these machines, might be major contributors to the overall noise level.

C. OBJECTIVES

The objectives of this thesis are to extend the analysis of piston slap, to confirm experimentally the analyses of this source, and to study other impacts, in order to better identify, understand, and predict the major noise sources in reciprocating machines. If the noise levels of reciprocating machines could be predicted by using easily obtainable engine or compressor parameters in emphirical formulas, the Navy could select the quietest machinery for use in its ships and submarines when analys-

ing bids from various suppliers. Also, if all major noise sources were properly understood, quieter reciprocating components could be designed.

Included in the thesis are the analysis of the effect on piston slap of wrist pin or crankshaft offset from the plane of piston cylinder axes as well as the analysis of valve and bearing slap impacts. Results are also included from a series of experiments with a single-cylinder diesel engine conducted with variations of the parameters which govern impacts.

II. PROCEDURE

A. ANALYSIS

The transverse motion of a piston, causing piston impacts, has been studied (19) using the dynamic and kinematic relations of a reciprocating machine. The same type of analysis has been carried out for the case when there is offset of the wrist pin or crankshaft from the plane of cylinder axes. From these analyses the impact velocities have been determined, and it was found that piston clearance, crank radius, machine speed, connecting rod length, cylinder gas pressure, offset, and mass of the internal components are the dominant factors effecting the severity of the piston impacts.

An analysis has been made of the bearing impacts, both main and connecting rod bearings, to see if they were of the same order of magnitude as the piston impacts. To do this the reactions at both bearings were calculated and plotted to see if there was any abrupt change in reaction vector direction. The whole vector had to be looked at in these cases because the motion is a rolling motion instead of reciprocating one like the piston experiences.

The velocity with which the valves seat on the cylinder head was calculated for a particular cam arrangement. This made it possible to compare these impact magnitudes with those caused by the piston and bearings.

B. MACHINE TESTED

Experiments were conducted on a diesel engine to verify the analysis. The engine used was a CFR single cylinder, four stroke, internal combustion engine that could be run as a diesel. It had a stroke of 4.50 inches and a bore of 3.25 inches and was equipped with overhead valves. It was located in the Experimental Projects Laboratory in the third wing of the

Massachusetts Institute of Technology. The engine was in a test cell so that other background noises could be eliminated. An electric motor was coupled to the engine so that it could be motored or run under load.

C. ENGINE PARAMETERS VARIED

For the engine used, the easiest parameters that could be varied to affect piston slap were piston clearance, speed, and cylinder gas pressure. Runs were conducted with pistons of different diameter installed which changed the piston clearance. These runs were made at various speeds from 800 RPM to 1400 RPM. The cylinder gas pressure was varied by both motoring and firing the engine. Vibration and acoustic data were obtained by using both an acceleration pickup and microphone, and the timing of the impacts with relation to crank angle was determined by using an oscilloscope from which pictures were obtained. In order to precisely obtain the timing of the piston slaps, an acceleration pickup was mounted inside one of the pistons. The lead was run down the connecting rod and out through an inspection plate. Oscilloscope pictures were taken at three speeds.

To determine the noise and vibrations caused by the valves, motoring runs were conducted at several speeds and several valve clearances. The same type runs were then made with the rocker arms lifted and the tappets held up by wire. The data from the two types of runs were then compared.

D. IMPACT SIMULATION

In order to simulate the impacts caused by the piston and valves, a ball bearing was dropped from various heights and pictures of the vibration peaks were taken on the oscilloscope. It was then possible to determine the kinetic energy of the impacts during the data runs by comparing the peak heights from the two sets of data.

Further details of procedure are found in Appendices A and B.

III. RESULTS

A. ANALYTICAL

1. Offset:

The normalized transverse force acting on a piston when there is offset of the wrist pin or crankshaft has been found* to be given by

$$\frac{F^{y}_{CP}(\Theta)}{M_P R\omega^2} \approx \Phi_G(\Theta) + \Phi_P(\Theta) + \Phi_C(\Theta), \tag{1}$$

where

$$\Phi_G(\Theta) \approx \Psi_G(\Theta)(\gamma \sin\Theta + \delta)$$

$$\Phi_P(\Theta) \approx -(\cos\Theta - \delta \sin\Theta + \gamma \cos 2\Theta)(\gamma \sin\Theta + \delta)$$

$$\Phi_C(\Theta) \approx -\mu\ell\left[(\cos\Theta - \frac{\delta\ell}{\gamma}\sin\Theta + \ell\gamma\cos 2\Theta)(\gamma\sin\Theta + \delta) + (1 - 2\ell - \frac{\rho^2}{\ell})\sin\Theta\right] .$$

Whenever the transverse force changes sign the piston begins to move across the clearance space and impacts against the cylinder liner. The transverse velocity of the piston at impact (19) is given by

$$V_o = R\omega\left[\frac{9}{2}\left(\frac{d}{R}\right)^2 K(\Theta_o)\right]^{1/3}, \tag{2}$$

and the crank angle changes by

$$\Delta\Theta = \left[\frac{6}{K(\Theta_o)}\left(\frac{d}{R}\right)\right]^{1/3} \tag{3}$$

as the piston transverses the clearance.

It has been found that

---

* See Appendix A for the development of the equations.

$$K(\Theta_o) \approx \Phi_G'(\Theta_o) + \Phi_P'(\Theta_o) + \Phi_C'(\Theta_o) \tag{4}$$

where

$$\Phi_G'(\Theta_o) \approx \frac{d\Psi_G(\Theta_o)}{d\Theta}(\gamma S + \delta) + \Psi_G(\Theta_o)\gamma C$$

$$\Phi_P'(\Theta_o) \approx (S + \delta C + 4\gamma SC)(\gamma S + \delta) - (C - \delta S + \gamma - 2\gamma S^2)\gamma C$$

$$\Phi_C'(\Theta_o) \approx \mu\ell\left[(S + \frac{\delta\ell C}{\gamma} + 4\ell\gamma SC)(\gamma S + \delta) - (C - \frac{\delta\ell S}{\gamma} + \ell\gamma - 2\ell\gamma S^2)\gamma C - (1 - 2\ell - \frac{\rho^2}{\ell})C\right],$$

and $S = \sin\Theta_o$, $C = \cos\Theta_o$, and Θ_o is the value of Θ where the right hand side of Eq.(1) equals zero.

Eq. 1 is plotted in Figure I for values of δ of + 0.05, 0.00, and - 0.05 for a typical four stroke diesel engine. From this figure one may deduce that a negative offset reduces the maximum transverse force (following TDC). Thus the magnitude of the most severe impact can be reduced by use of a negative offset. Positive offset has the opposite effect, it tends to aggravate TDC impacts.

2. Bearing Slap:

The normalized x and y force components acting on the connecting rod bearing sleeve have been found to be given by

$$\frac{F^x_{RC}(\Theta)}{M_P R\omega^2} = \Phi_{G_1}(\Theta) + \Phi_{P_1}(\Theta) + \Phi_{C_1}(\Theta)$$

and

$$\frac{F^y_{RC}(\Theta)}{M_P R\omega^2} = \Phi_{G_2}(\Theta) + \Phi_{P_2}(\Theta) + \Phi_{C_2}(\Theta) \tag{5}$$

FIGURE I

Effect of Offset on Transverse Force Acting on the Piston.

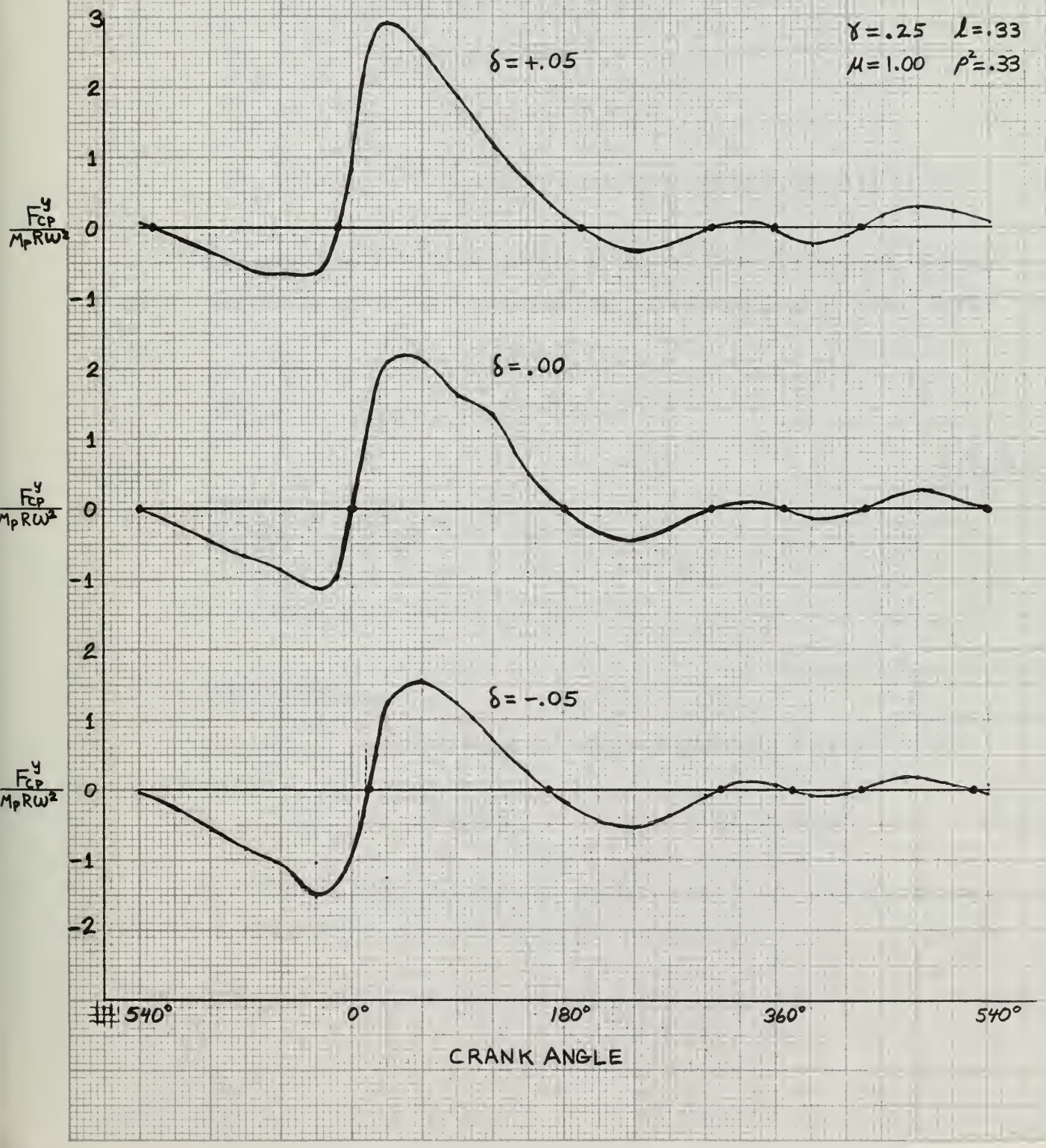

respectively, where

$$\Phi_{G_1}(\Theta) = \Psi_G(\Theta)$$

$$\Phi_{P_1}(\Theta) = -(\cos\Theta + \gamma\cos 2\Theta)$$

$$\Phi_{C_1}(\Theta) = -\mu(\cos\Theta + \gamma\ell\cos 2\Theta)$$

$$\Phi_{G_2}(\Theta) \approx -\Psi_G(\Theta)\,\gamma\sin\Theta$$

$$\Phi_{P_2}(\Theta) \approx (\cos\Theta + \gamma\cos 2\Theta)\,\gamma\sin\Theta$$

$$\Phi_{C_2}(\Theta) \approx \mu\left[-\frac{(1-\ell)^2 - \rho^2}{\gamma} + \ell\cos\Theta + \gamma(\ell^2+\rho^2)\cos 2\Theta\right]\gamma\sin\Theta$$

The normalized force components acting on the main bearing journals differ from those acting on the connecting rod bearings by only the inertia force of the crank. Thus,

$$\frac{F_A^x}{M_P R\omega^2} = \frac{F_{RC}^x}{M_P R\omega^2} - \nu\lambda\cos\Theta$$

and (6)

$$\frac{F_A^y}{M_P R\omega^2} = \frac{F_{RC}^y}{M_P R\omega^2} - \nu\lambda\sin\Theta$$

Eqs.(5) and (6) are plotted in Figure II.

3. Valve Impacts:

The velocity $\dot{y}$ of the valve as it impacts against its seat was found to be given by*

$$\dot{y} = \frac{\omega}{\cos^2\Theta}(a\sin\Theta + b), \qquad (7)$$

where Θ is the camshaft angle at which the valve seats. This is measured from the position where the straight segment of the cam is tangent to

---

* This is for the particular cam and tappet arrangement of the engine tested.

FIGURE II

Connecting Rod and Main Bearing Reaction Components

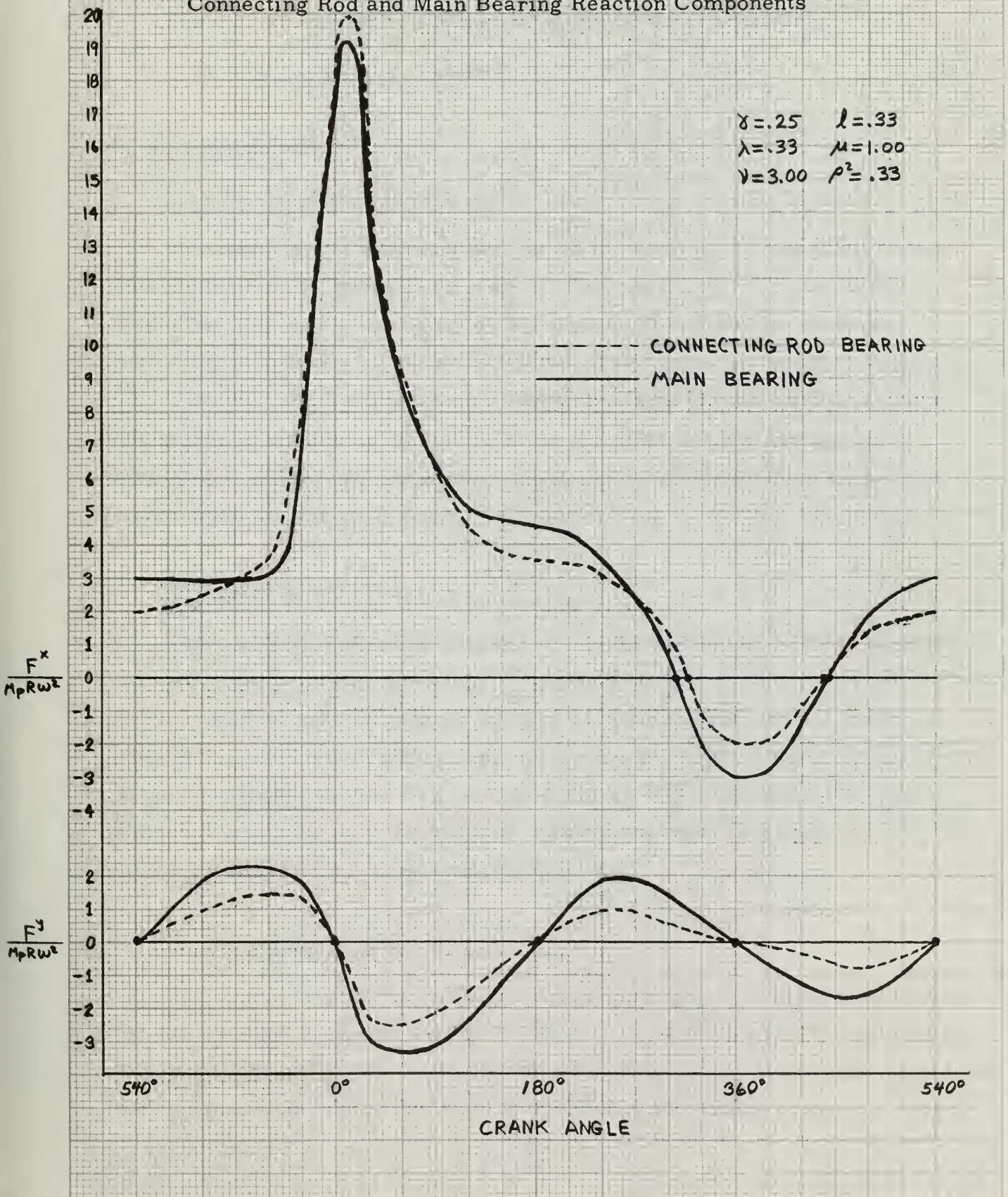

the tappet base.

For a given clearance setting, d, Θ can be determined from

$$(a + d) \cos \Theta = a + b \sin \Theta \qquad (8)$$

B. EXPERIMENTAL:

1. Effect of Piston Clearance

Increased piston clearance was found to result in increased vibration and radiated noise levels of the engine. Figures III, IV, V, and VI show this effect for fueled operation of the engine. Piston slap is dominant primarily at frequencies between 400 and 4000 cycles per second. Figures VII, VIII, IX, and X show piston clearance effects for the condition where the engine is motored with rocker arms and tappets lifted (compressor simulation). Figure XI shows the timing and the peak vibration levels obtained when the piston clearance is changed from 0.002 to 0.011 inches.

2. Engine Speed Effect:

The vibration and radiated noise levels were found to be more dependent on speed than on piston clearance. Figures XII, XIII, XIV, and XV show these levels for speeds between 800 and 1400 RPM. The overall levels when firing were 10 db higher than when the engine was motored with rocker arms and tappets lifted. By comparing Figure XVI with the bottom half of Figure XI one may note the effect of a speed increase from 800 to 1000 RPM on the timing and on the peak vibration levels.

3. Combustion Effect and Valve Noise:

The overall vibratory levels for firing were only 1 db higher than those for the motored engine as evidenced from Figures XVII and XVIII. However, this small change is due to the dominance of valve noise above 5000 cycles per second. Combustion had a greater effect in the middle frequency range.

Figure III. Vibration Levels at Various Piston Clearances; Engine Fired at 1000 RPM.

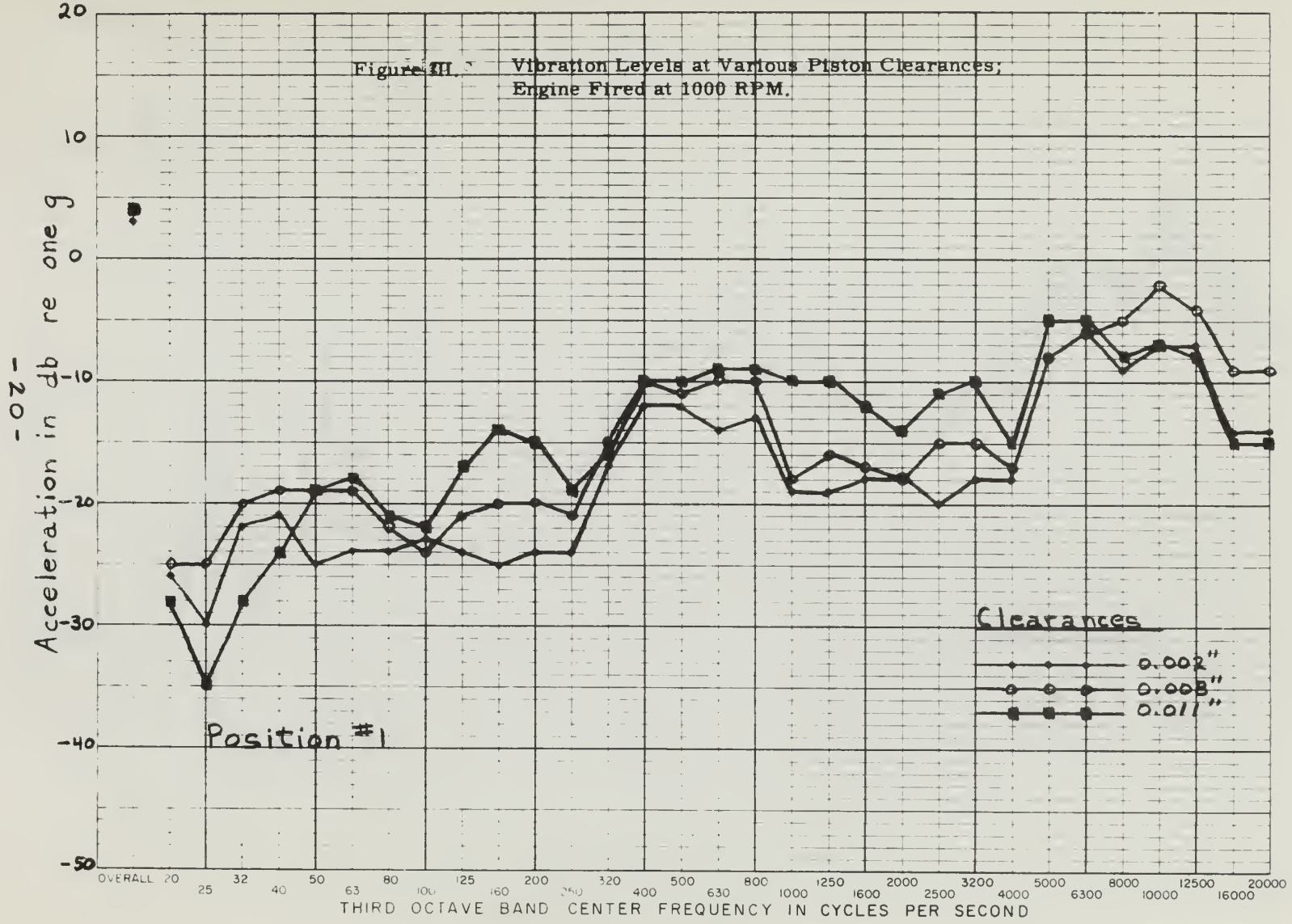

Figure IV. Vibration Levels at Various Piston Clearances; Engine Fired at 1400 RPM.

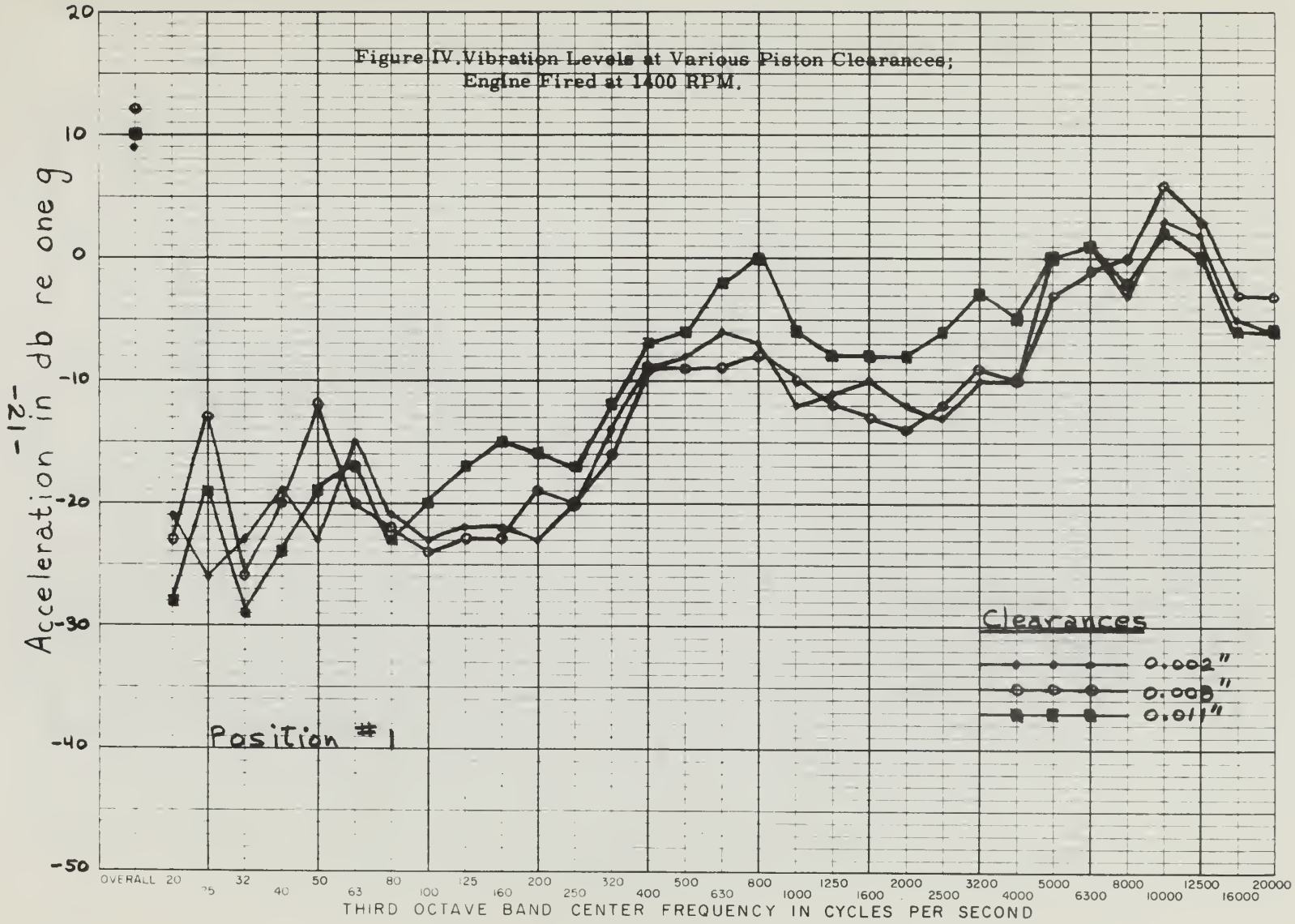

Figure V. Radiated Noise Levels at Various Piston Clearances; Engine Fired at 1000 RPM.

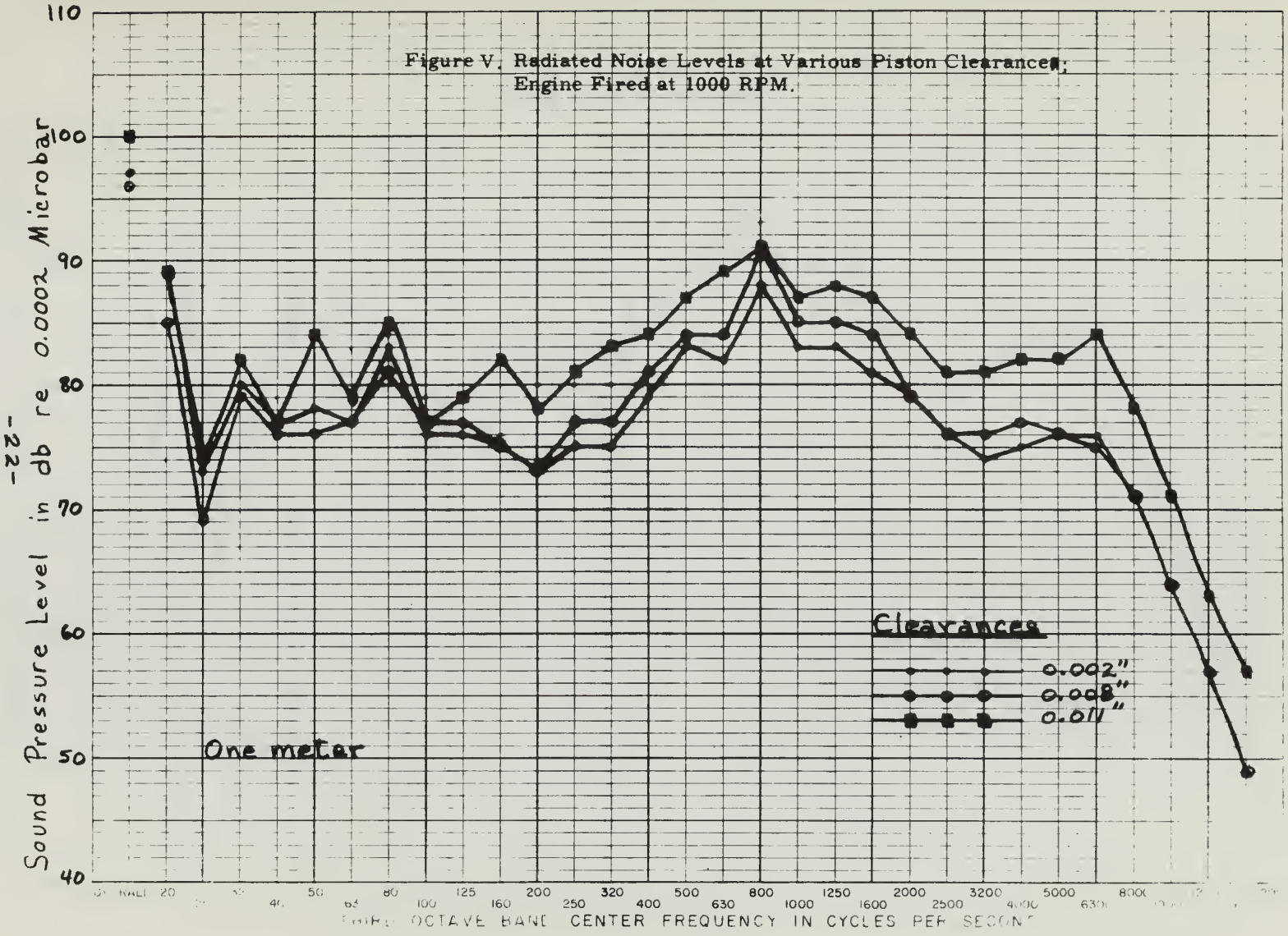

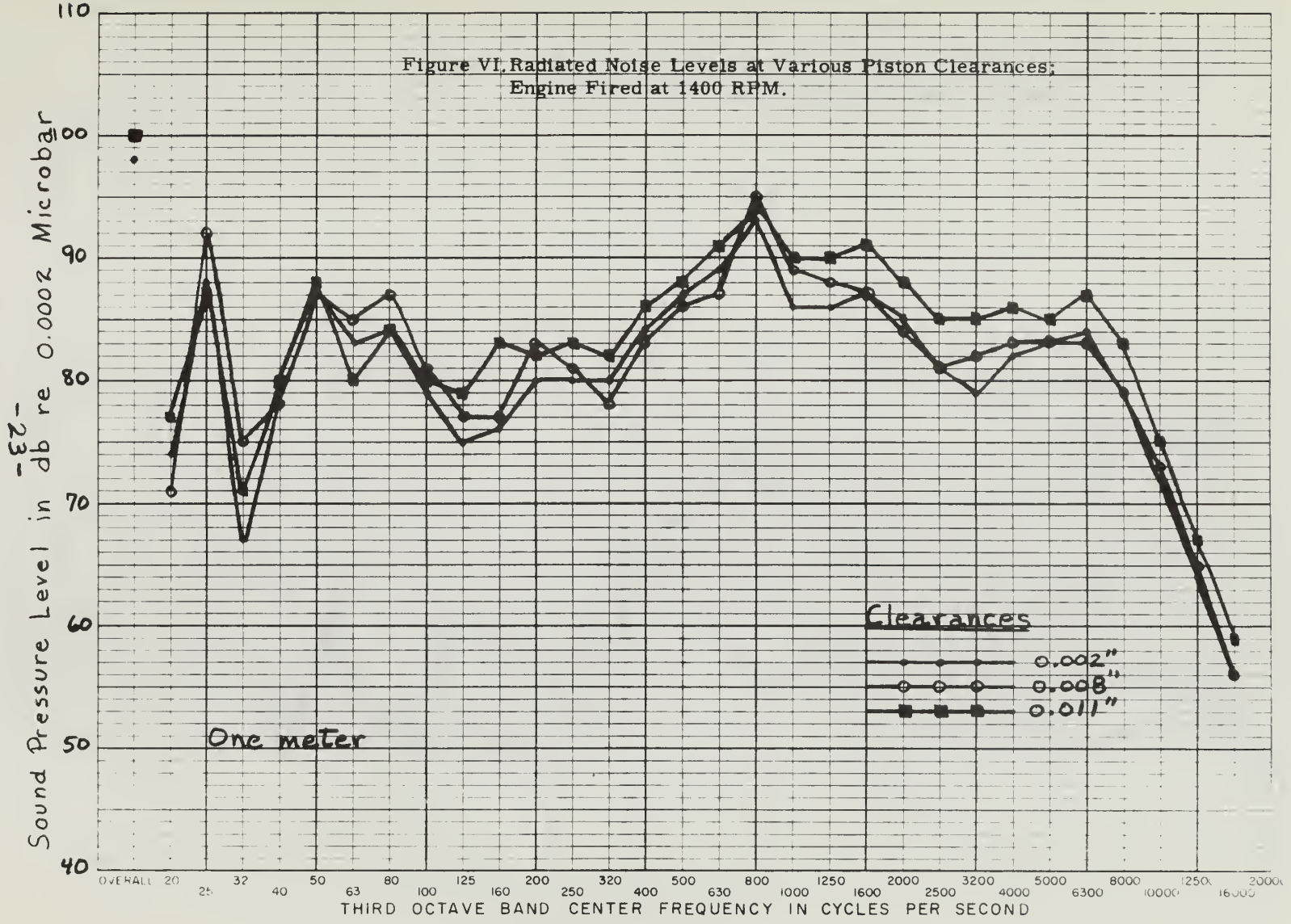
Figure VI. Radiated Noise Levels at Various Piston Clearances; Engine Fired at 1400 RPM.
Sound Pressure Level in db re 0.0002 Microbar
110
100
90
80
70
60
50
40
Clearances
0.002"
0.008"
0.011"
One meter
OVERALL
20
25
32
40
50
63
80
100
125
160
200
250
320
400
500
630
800
1000
1250
1600
2000
2500
3200
4000
5000
6300
8000
10000
12500
16000
20000
THIRD OCTAVE BAND CENTER FREQUENCY IN CYCLES PER SECOND

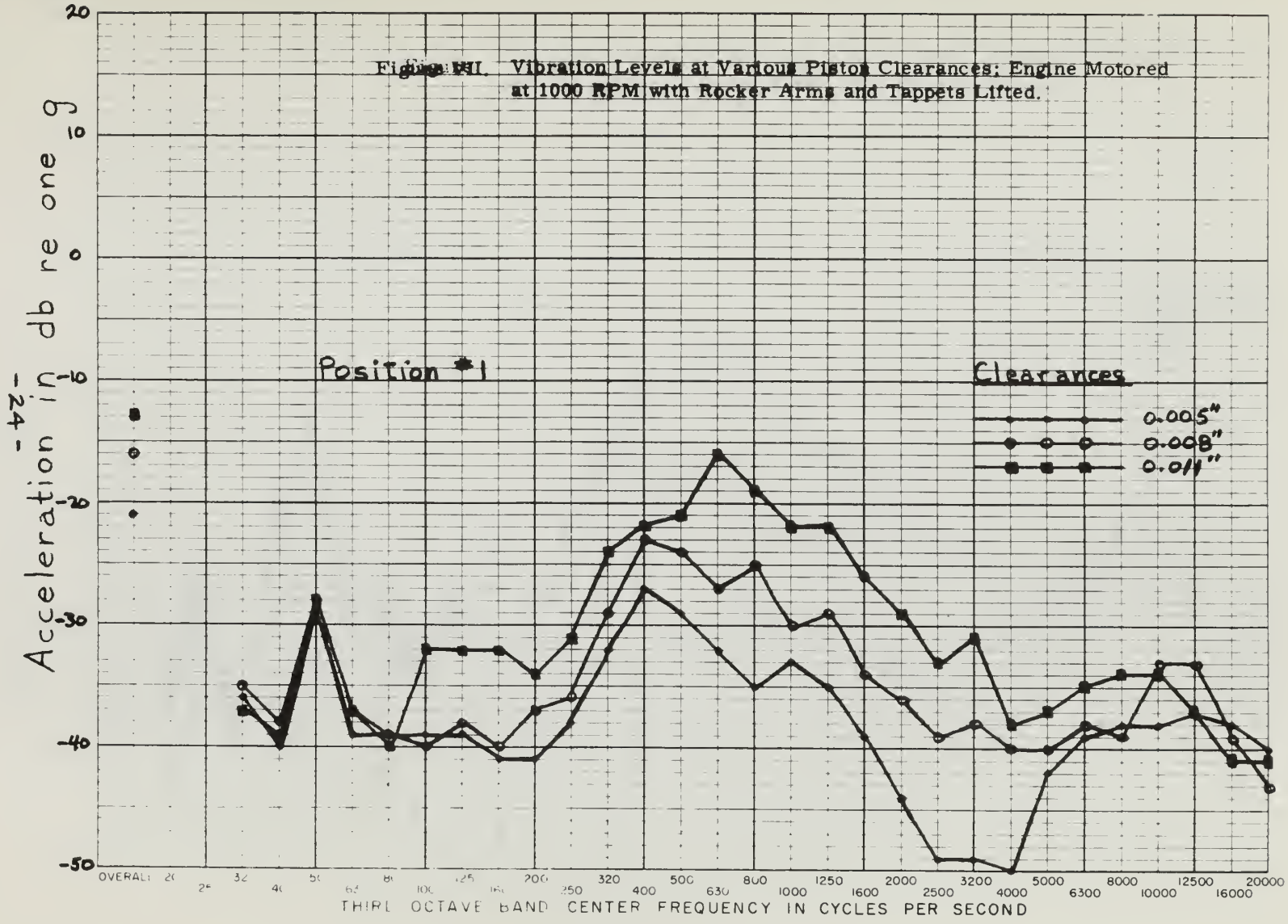

Figure VII. Vibration Levels at Various Piston Clearances; Engine Motored at 1000 RPM with Rocker Arms and Tappets Lifted.

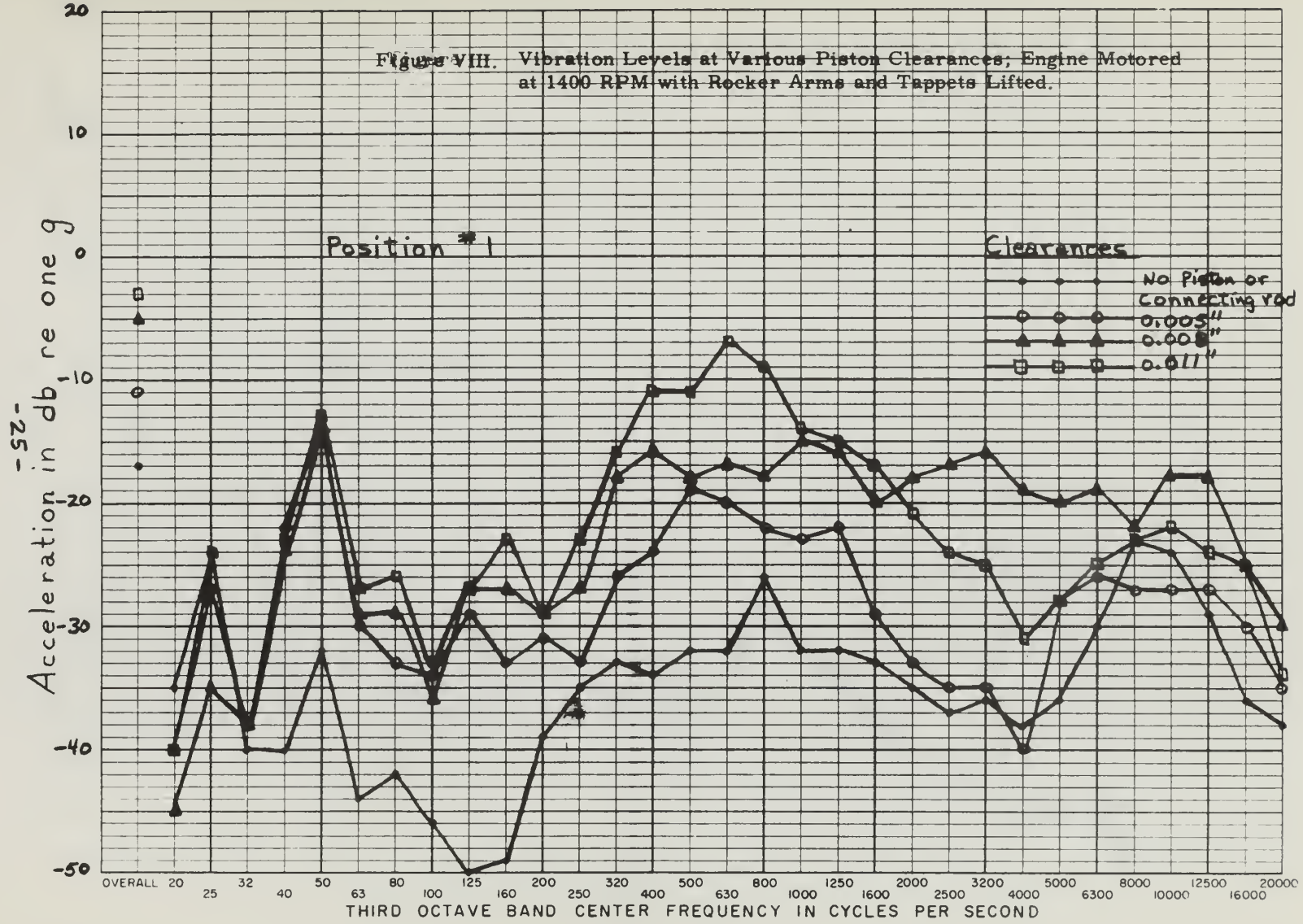

Figure VIII. Vibration Levels at Various Piston Clearances; Engine Motored at 1400 RPM with Rocker Arms and Tappets Lifted.

Figure IX. Radiated Noise Levels at Various Piston Clearances; Engine Motored at 800 RPM with Rocker Arms and Tappets Lifted.

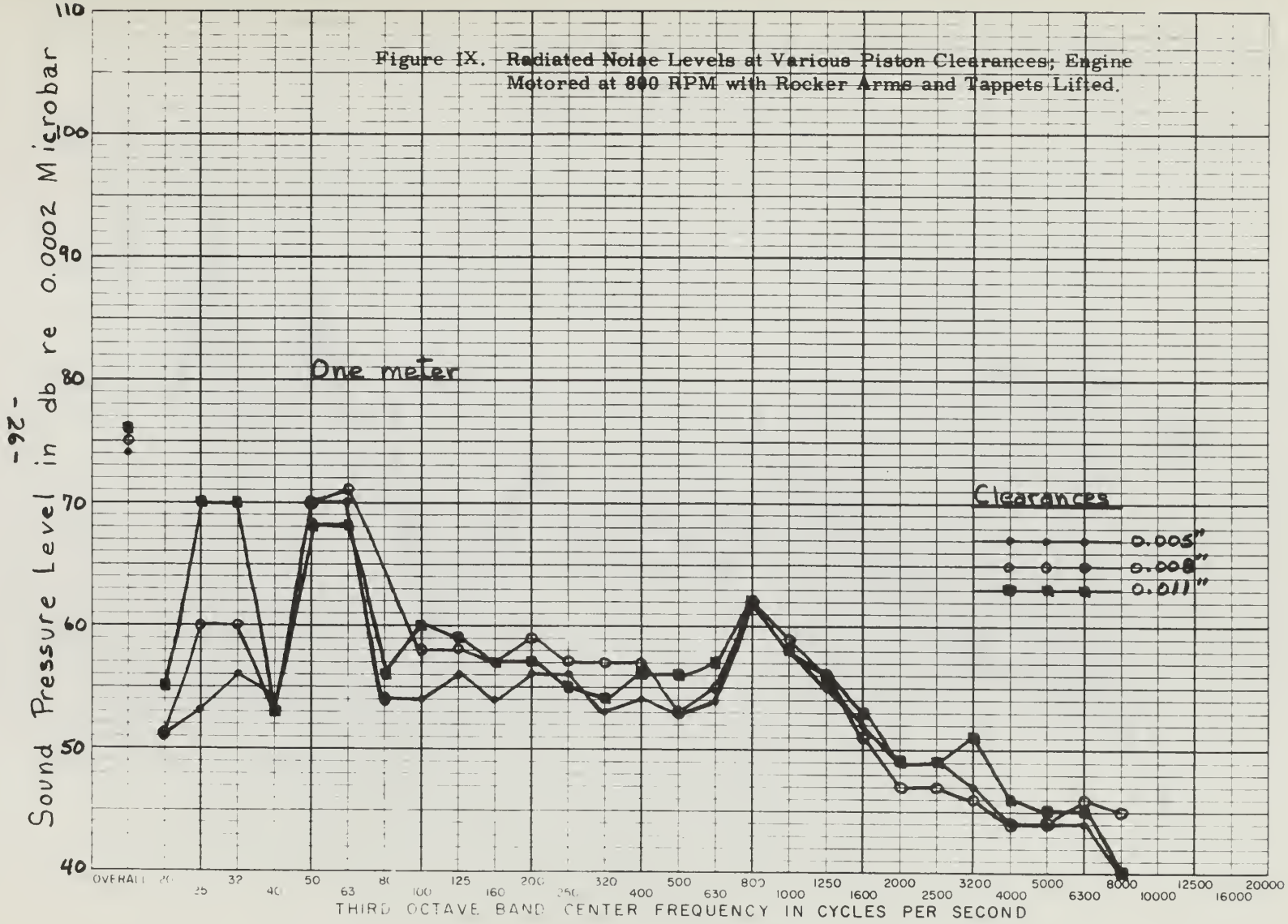

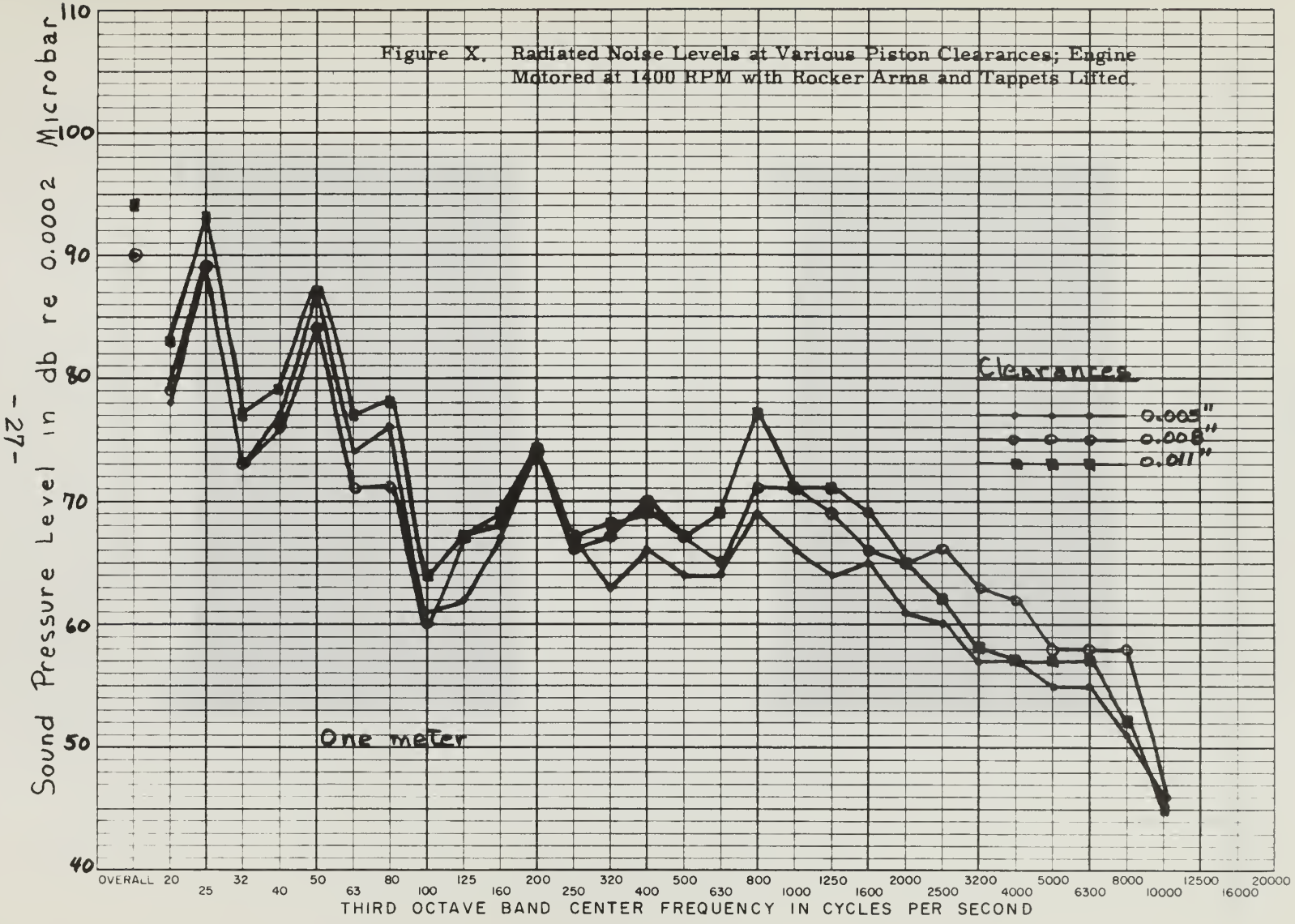

Figure X. Radiated Noise Levels at Various Piston Clearances; Engine Motored at 1400 RPM with Rocker Arms and Tappets Lifted.

Figure XI.

Peak Vibration Levels vs. Crank Angle; Engine Fired at 800 RPM.

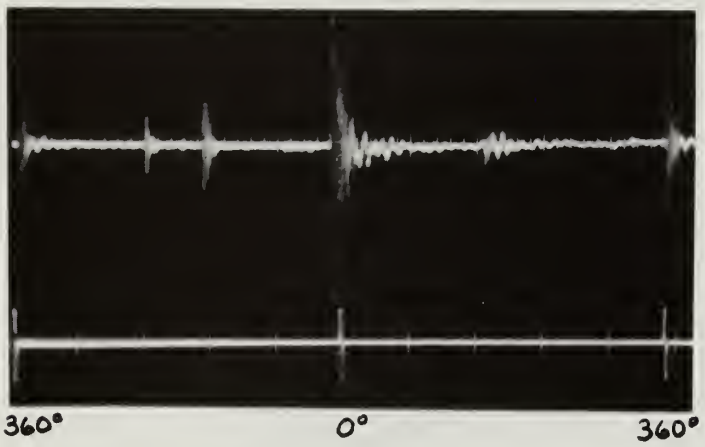

0.002 inch Piston Clearance

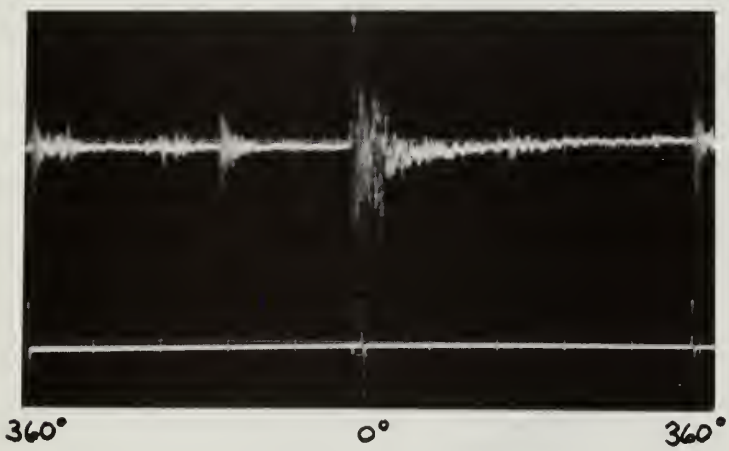

0.011 inch Piston Clearance

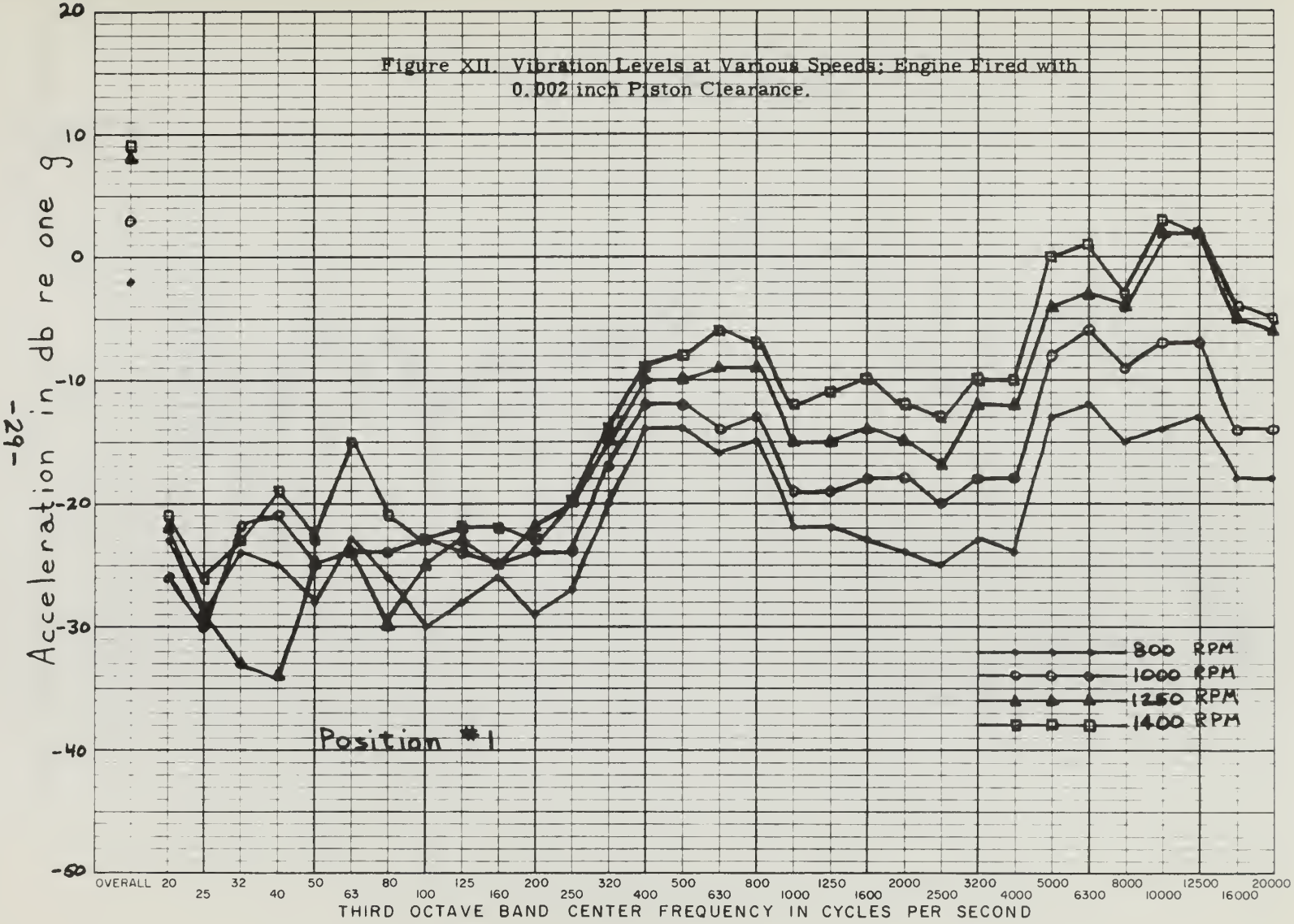

Figure XII. Vibration Levels at Various Speeds; Engine Fired with 0.002 inch Piston Clearance.

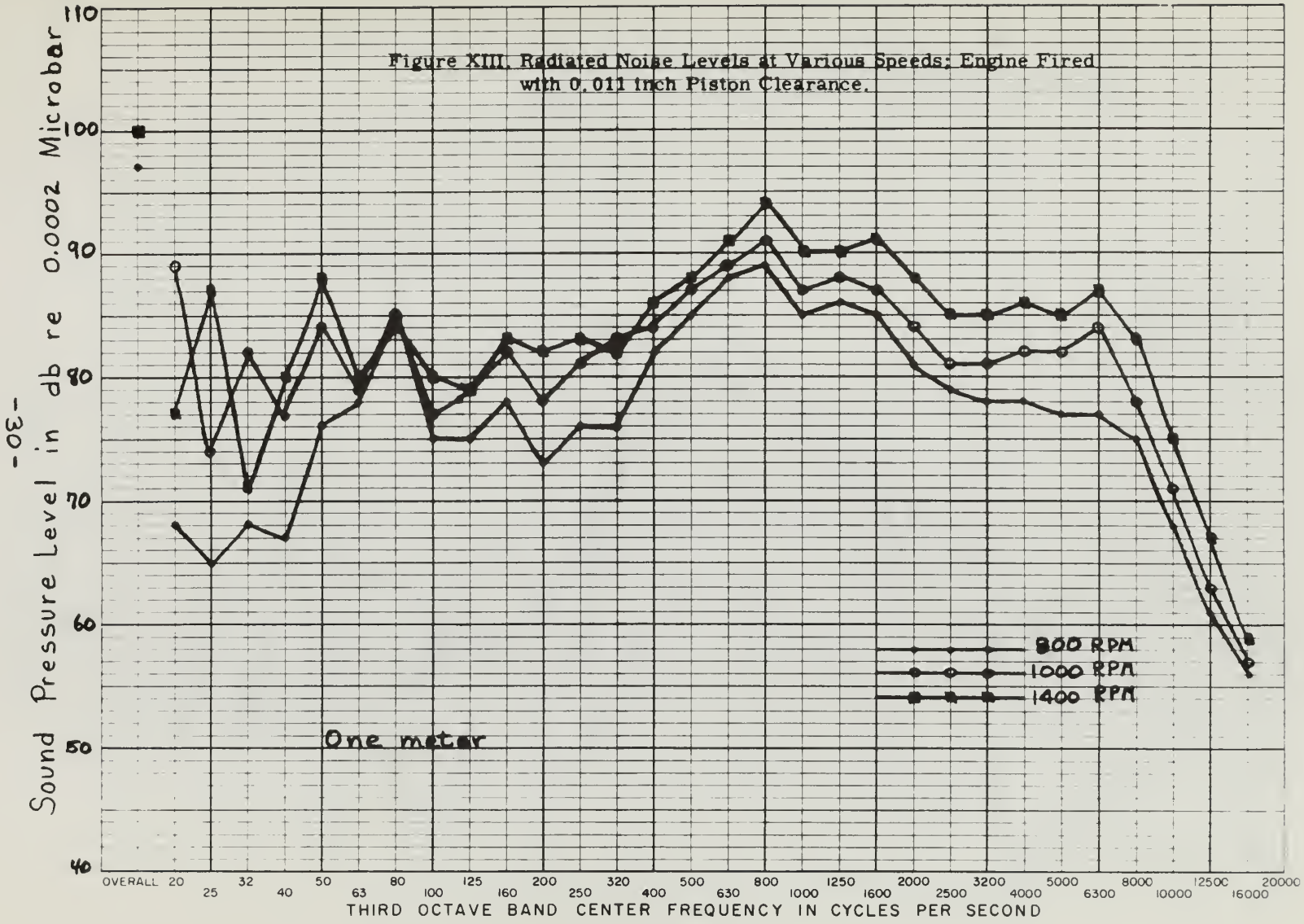
Figure XIII. Radiated Noise Levels at Various Speeds: Engine Fired with 0.011 Inch Piston Clearance.
Sound Pressure Level in db re 0.0002 Microbar
110
100
90
80
70
60
50
40
800 RPM
1000 RPM
1400 RPM
One meter
OVERALL 20 25 32 40 50 63 80 100 125 160 200 250 320 400 500 630 800 1000 1250 1600 2000 2500 3200 4000 5000 6300 8000 10000 12500 16000 20000
THIRD OCTAVE BAND CENTER FREQUENCY IN CYCLES PER SECOND

Figure XIV. Vibration Levels at Various Speeds; Engine Motored with 0.011 inch Piston Clearance and Rocker Arms and Tappets Lifted.

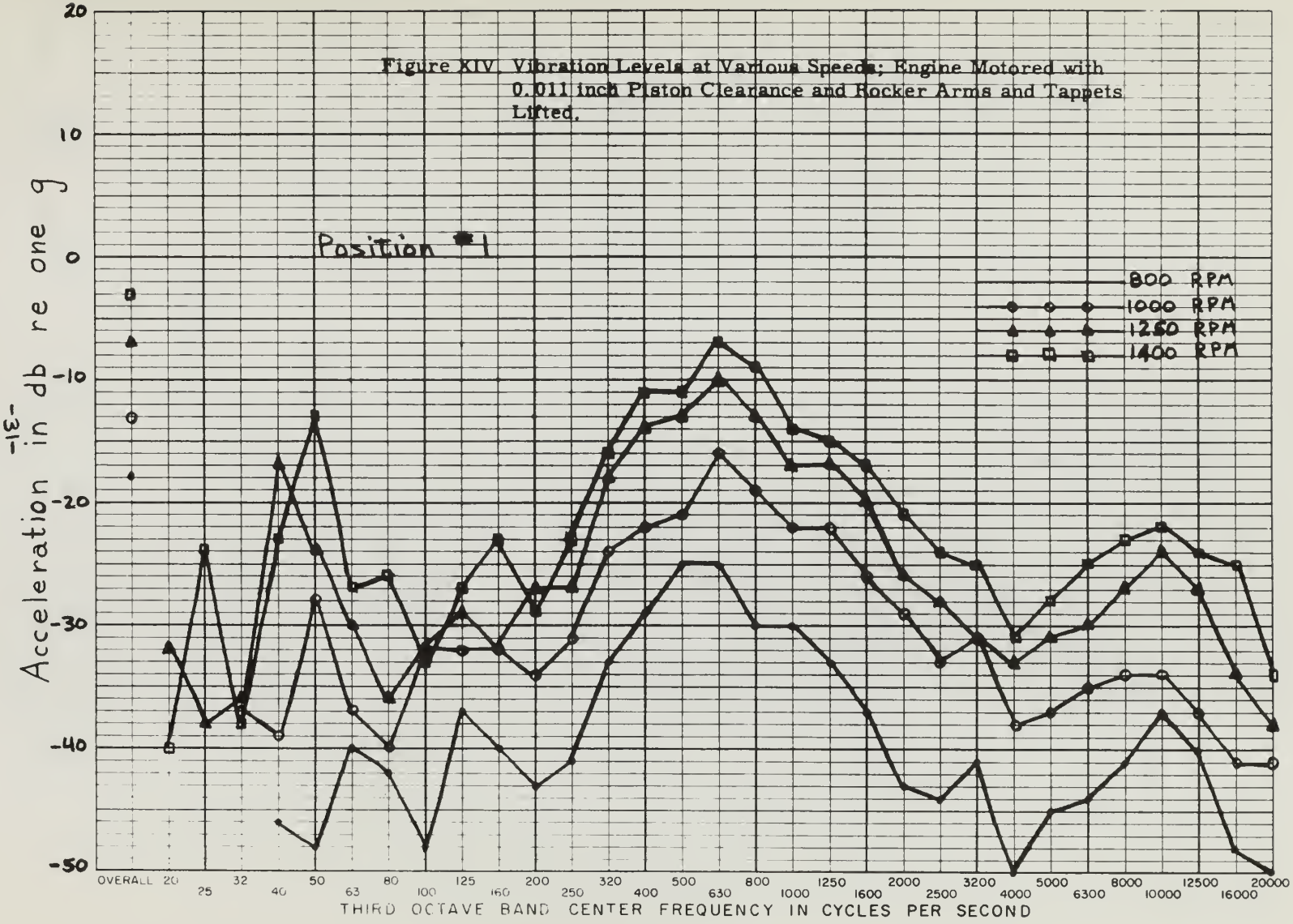

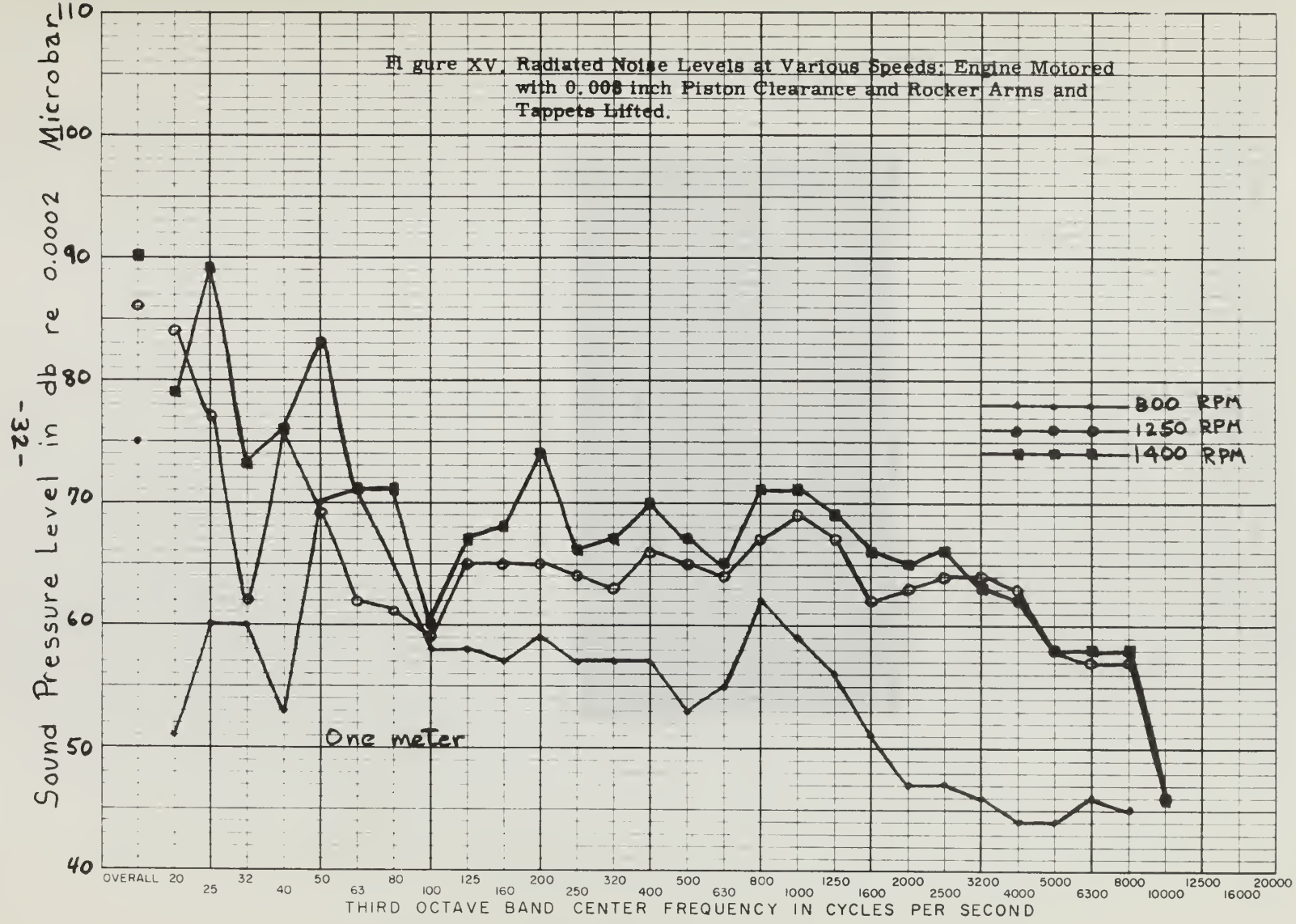
Figure XV. Radiated Noise Levels at Various Speeds: Engine Motored with 0.008 inch Piston Clearance and Rocker Arms and Tappets Lifted.
Sound Pressure Level in db re 0.0002 Microbar
110
100
90
80
70
60
50
40
800 RPM
1250 RPM
1400 RPM
One meter
OVERALL 20 25 32 40 50 63 80 100 125 160 200 250 320 400 500 630 800 1000 1250 1600 2000 2500 3200 4000 5000 6300 8000 10000 12500 16000 20000
THIRD OCTAVE BAND CENTER FREQUENCY IN CYCLES PER SECOND

Figure XVI.

Peak Vibration Levels vs. Crank Angle; Engine Fired at 1000 RPM and 0.011 inch Piston Clearance.

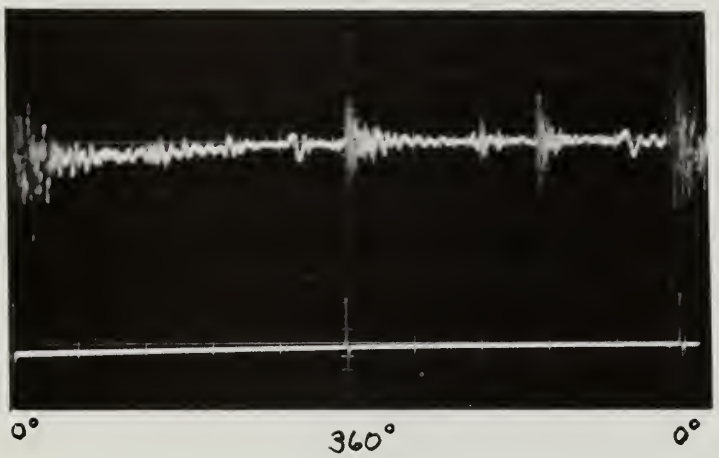

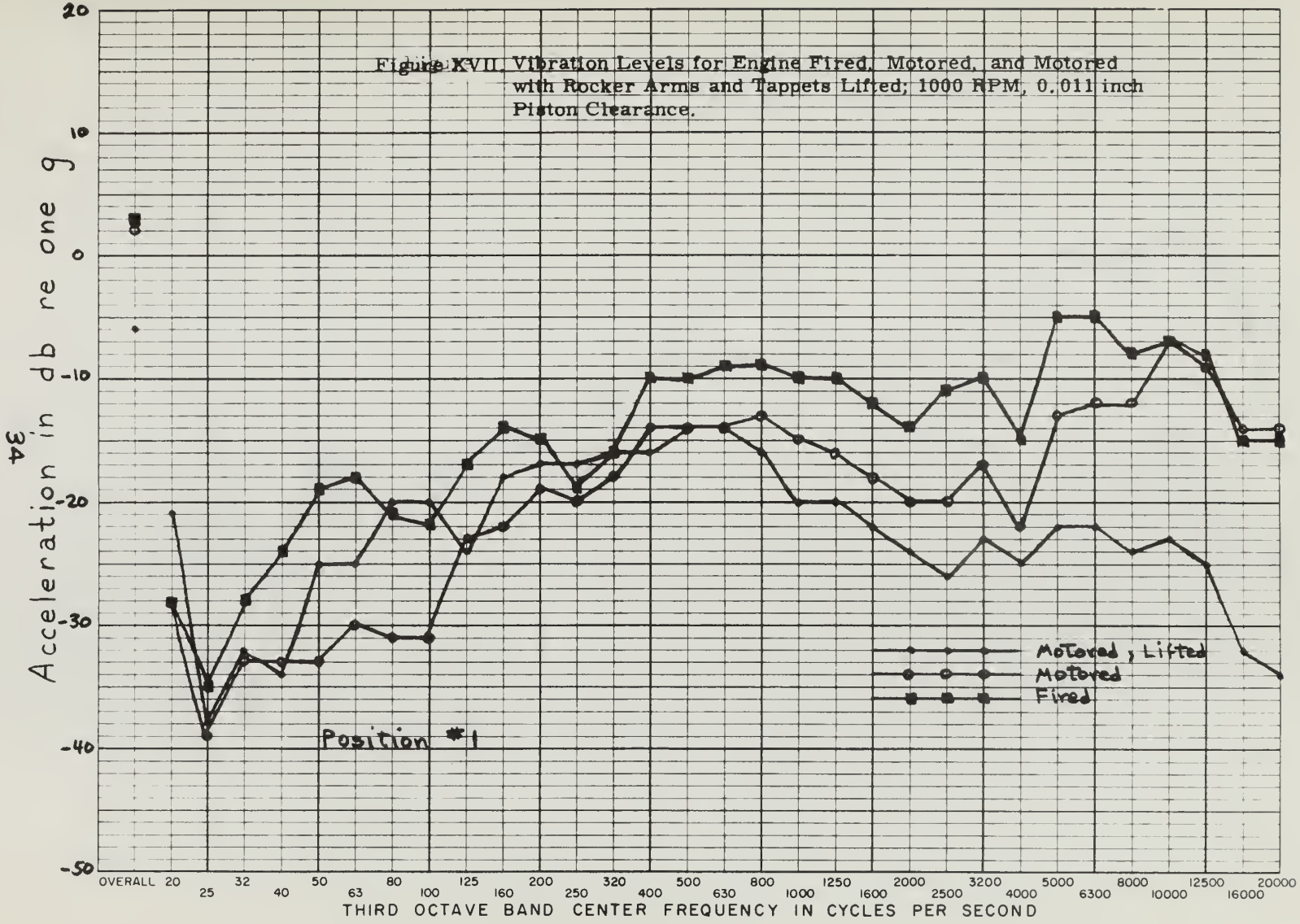

Figure XVII. Vibration Levels for Engine Fired, Motored, and Motored with Rocker Arms and Tappets Lifted; 1000 RPM, 0.011 inch Piston Clearance.

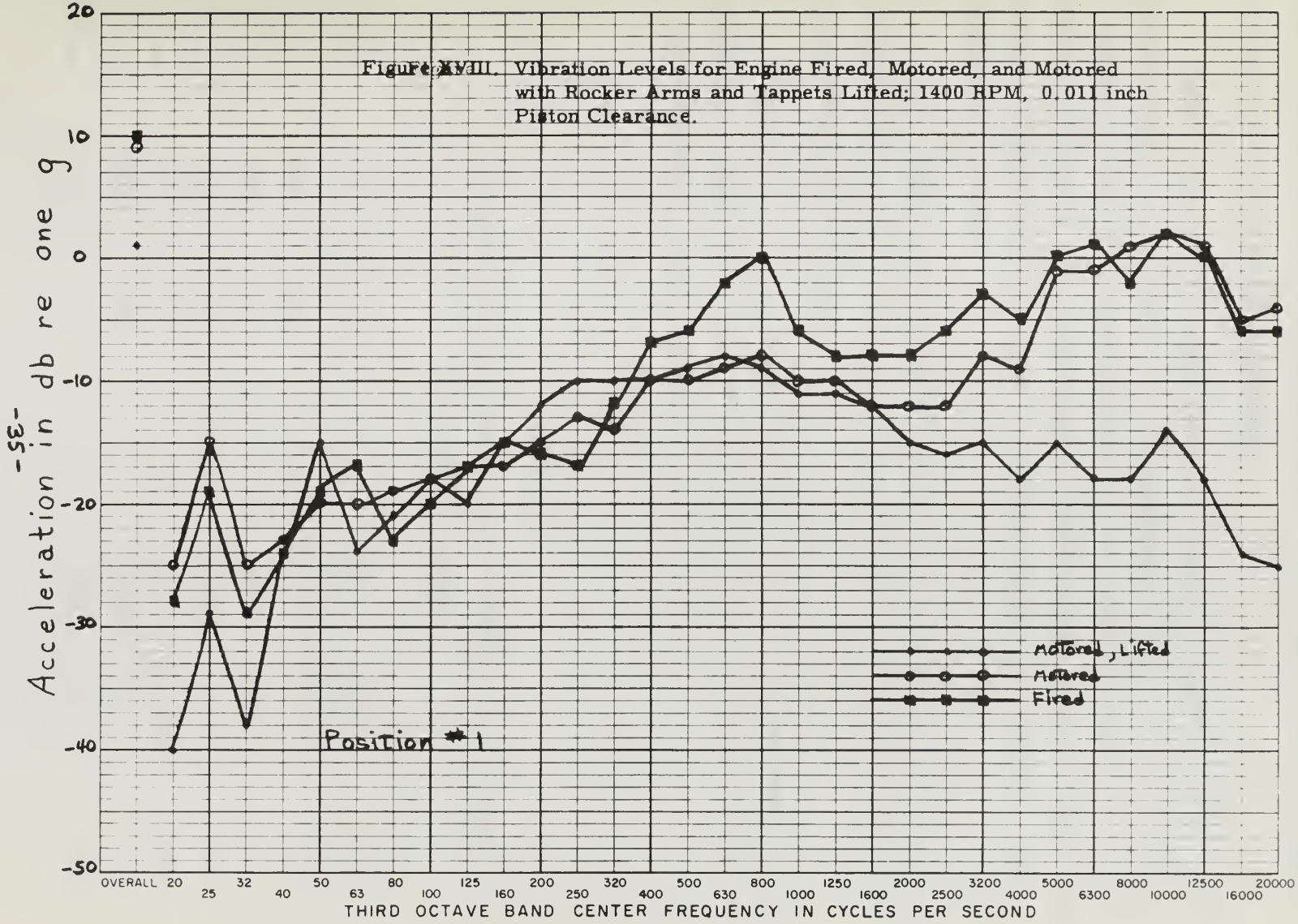
Figure XVIII. Vibration Levels for Engine Fired, Motored, and Motored with Rocker Arms and Tappets Lifted; 1400 RPM, 0.011 inch Piston Clearance.
Acceleration in db re one g
20
10
0
-10
-20
-30
-40
-50
Motored, Lifted
Motored
Fired
Position #1
OVERALL 20 25 32 40 50 63 80 100 125 160 200 250 320 400 500 630 800 1000 1250 1600 2000 2500 3200 4000 5000 6300 8000 10000 12500 16000 20000
THIRD OCTAVE BAND CENTER FREQUENCY IN CYCLES PER SECOND

When the valve rocker arms and tappets were lifted the high frequency levels were decreased considerably.

Figures XIX and XX show that combustion has a greater effect on the radiated noise levels than on the vibration levels. Once again the high frequency levels drop when the valve rocker arms and tappets are lifted. Figure XXI shows the timing and the peak vibration levels for the three cases of firing, motoring, and motoring with rocker arms and tappets lifted at 1250 RPM.

Figure XXII shows the impacts experienced by the piston as a function of crank angle, for the motored engine, obtained from an accelerometer mounted inside the piston.

A summary of the comparison of calculated and experimental values of kinetic energy and $\Delta\Theta$ for the piston are given in Table I. A comparison for valve impact kinetic energies is given in Table II.

TABLE I

Calculated and Experimental Values of Kinetic Energy and $\Delta\Theta$ for Piston Impacts

Type	RPM	Clearance	Cal. K.E.	Exp. K.E.	Cal. $\Delta\Theta$	Exp. $\Delta\Theta$
Motored	800	.008	.060	.0013	10.8°	19°
Motored	1000	.011	.095	.0012	14.1°	31°
Fired	1000	.002	.020	.0014	5.7°	14°
Fired	800	.008	.115	.0037	7.8°	20°
Fired	1400	.008	.161	.0038	11.5°	12°
Fired	1400	.011	.244	.0026	12.8°	14°

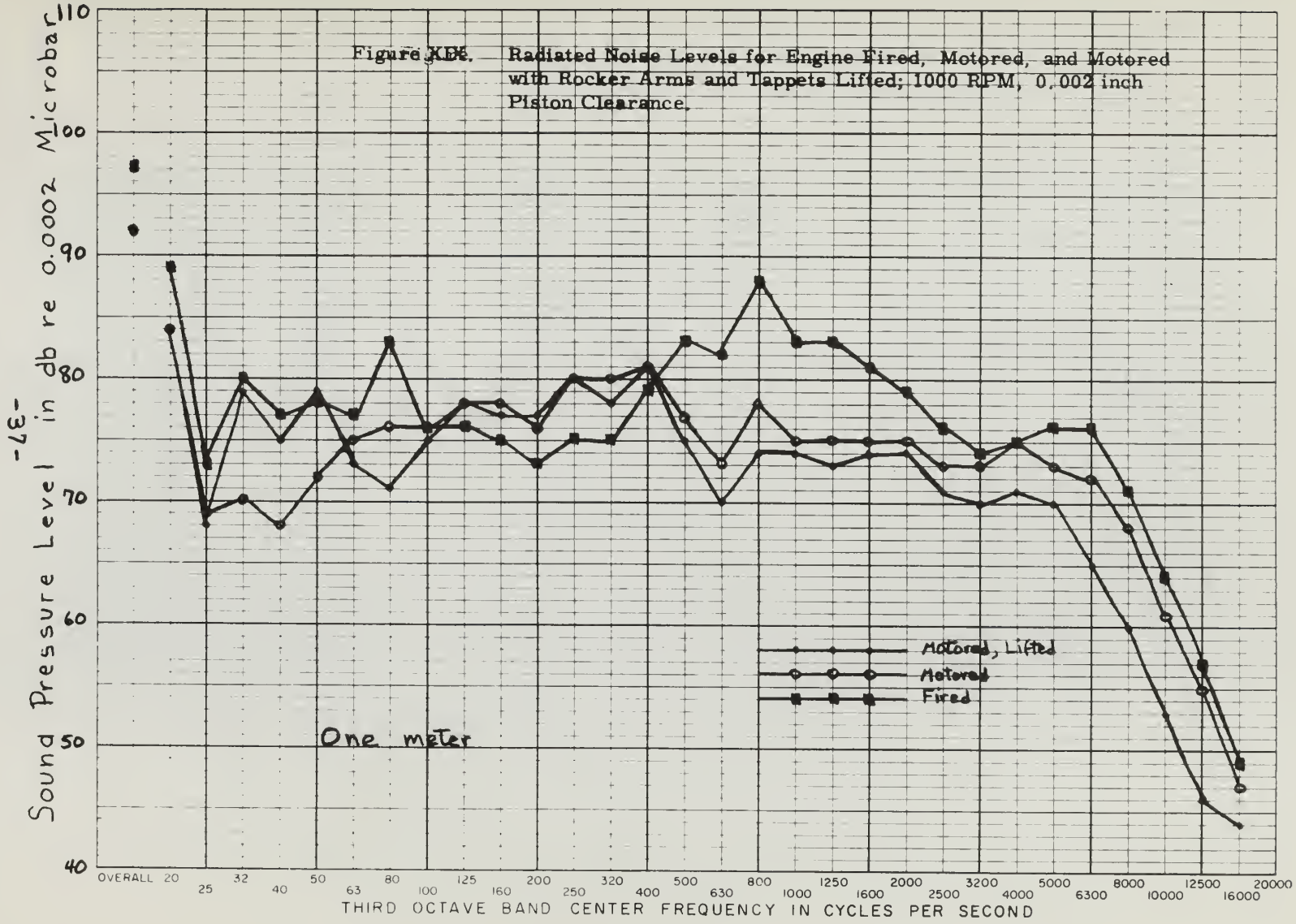

Figure XIII. Radiated Noise Levels for Engine Fired, Motored, and Motored with Rocker Arms and Tappets Lifted; 1000 RPM, 0.002 inch Piston Clearance.

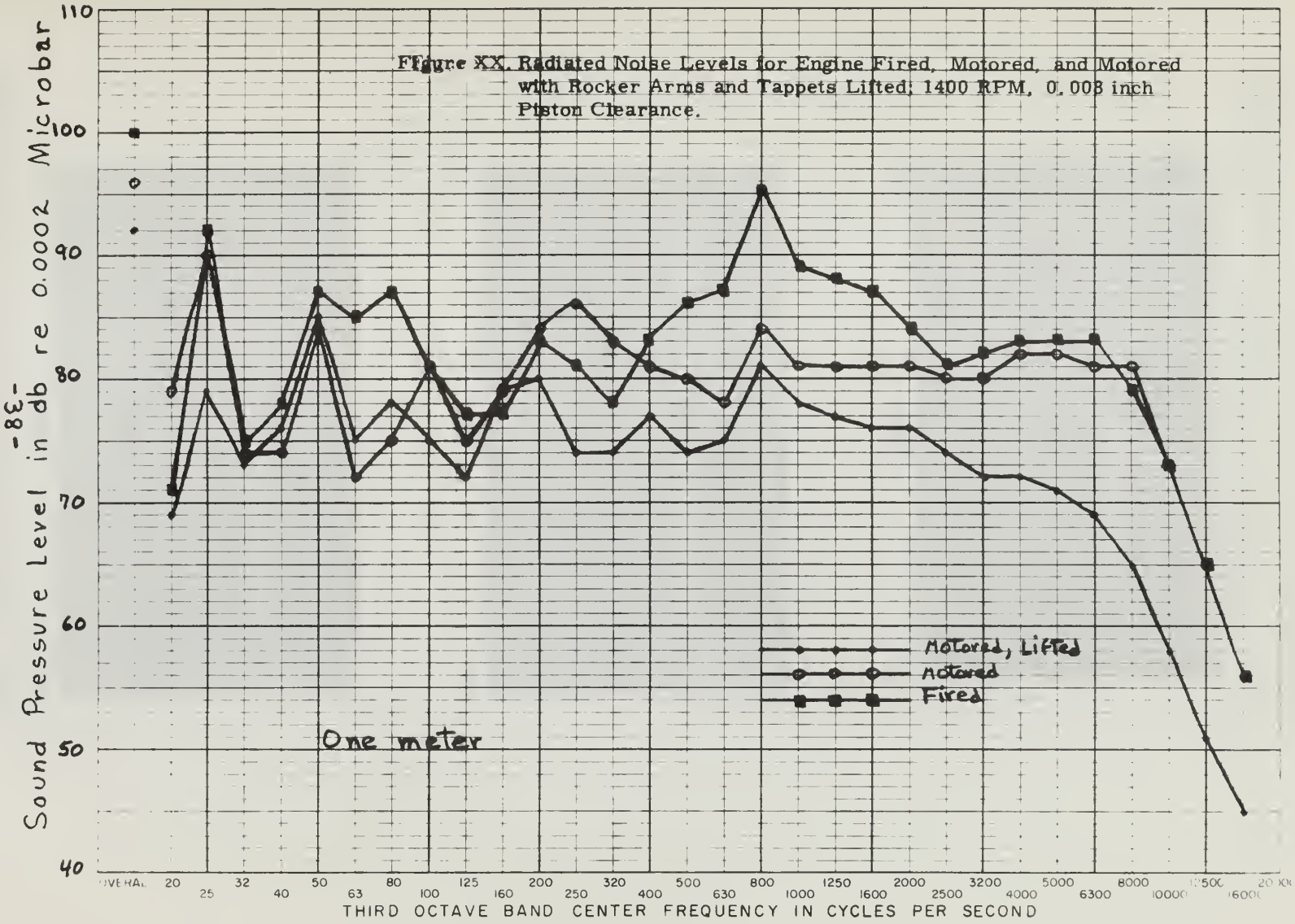

Figure XX. Radiated Noise Levels for Engine Fired, Motored, and Motored with Rocker Arms and Tappets Lifted; 1400 RPM, 0.003 inch Piston Clearance.

Figure XXI.

Peak Vibration Levels vs. Crank Angle; 1250 RPM and 0.008 inch Piston Clearance.

Engine Fired

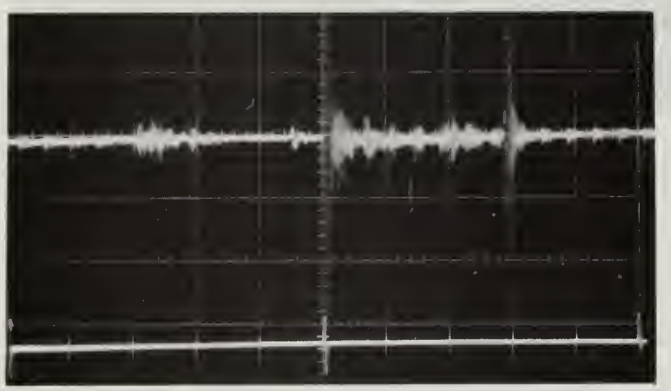

En gine Motored

Engine Motored with Rocker Arms and Tappets Lifted

Figure XXII.

Peak Vibration Levels vs. Crank Angle with Pickup Mounted in the Piston; Engine Motored at 1000 RPM and 0.008 inch Piston Clearance.

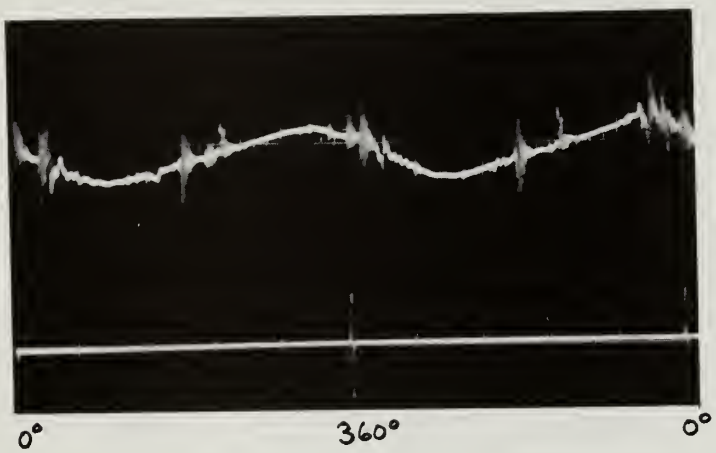

TABLE II

Calculated and Experimental Values of Kinetic Energy for Valve Impacts

RPM	Clearance	Valve	Cal. K.E.	Exp. K.E.
800	.010	Exh.	.017	.009
1000	.010	Exh.	.026	.016
1250	.010	Exh.	.041	.021
1600	.010	Exh.	.068	.031
1000	.006	Int.	.016	.009
1000	.008	Int.	.016	.014
1000	.012	Int.	.016	.018
1000	.015	Int.	.016	.027
1000	.020	Int.	.016	.039

IV. DISCUSSION OF RESULTS

A. EFFECT OF OFFSET

Figure I shows that the maximum transverse force following a change in sign occurs following TDC of the power stroke (0 degrees crank angle). This then is where the most severe piston impact would occur. A negative offset* decreases the magnitude of the transverse force and would reduce piston slap. Figure I is plotted for δ equal to 0.05 which is a one-half inch offset for a connecting rod length of ten inches. For this case the transverse force is reduced by about 30% which is about a 25% reduction in impact kinetic energy. Although $\delta = 0.05$ is a fairly large offset, smaller values would still be useful in reducing the heaviest impact.

Positive offset should not be used in a reciprocating machine as it would increase the magnitude of the power stroke impact and unnecessarily increase the noise and vibration levels.

B. OCCURENCE OF BEARING SLAP

The magnitude of the x-direction** reactions at both the connecting rod and main bearings is very large around 0 degrees crank angle as seen in Figure II. However, there is no change in the sign of the reaction in this vicinity and thus no tendency for the bearing to slap. The x-direction reactions around 360 degrees crank angle and the y-direction reactions do have sign changes. There is, however, no abrupt change in the total reaction vector as none of these sign changes occur concurrently. Thus the motion of the journal in the sleeve would be more of a rolling and sliding

---

*) Figure A-I defines negative offset.

**) Directions are defined in Figure A-I.

motion. This plus the fact that the bearing clearances are small would indicate that any bearing slaps would be of lower magnitude than the piston impacts.

The possibility of an impact at the wrist pin was not studied as the motion of the pin inside the piston is very complicated. Also, the clearance is very small so that the impacts could not be too severe.

C. COMPARISON OF KINETIC ENERGIES

As seen in Table I, the kinetic energies of the piston at impact calculated using Eq.(2) were very much larger than the kinetic energies of the ball bearing used during impact simulation. The calculated value varied from about 15 to 95 times the experimental value. Likewise the values of $\Delta\Theta$ calculated using Eq.(3) were in all cases less than the crank angle at impact read from the oscilloscope pictures. The computed values varied from .39 to .94 of the experimental values.

A logical explanation for such large discrepancies is that the piston ring friction and canting of the piston have a much larger effect on the impacts than at first suspected. Both of these phenomenon were omitted from the original theory (19). If the friction between the piston and its rings was significant, there would be a substantial force retarding the transverse motion of the piston. This would both decrease the kinetic energy at impact and increase the time of piston transit which increases $\Delta\Theta$. Also, the canting of the piston around the wrist pin would change the time of piston transit as well as reduce the effective mass at impact. During engine operation there was also a great deal of lubricating oil flowing out around the lower rings. This oil would also tend to damp the motion of the piston.

The clearances used in the calculations for kinetic energy were the cold measured clearances. Although the engine was run very cold in order

to maintain the original clearances, there would have been some heating and expansion of the piston.

The calculated values of valve impact kinetic energy with proper clearance setting agreed fairly well with the simulated values. The calculations, using Eq.(7), gave values of from 1.6 to 2.2 times the experimentally found ones. This would show that there was some damping in the valve linkage which retarded the motion. Eq.(7) and (8) did not, however, adequately account for the change in valve clearance settings. As d was changed from 0.006 to 0.020 inches, Eq.(8) gave the value of Θ as changing from 1 to 2 degrees. When this change was used in Eq.(7) the change in kinetic energy was negligible. More study is necessary to determine the exact phenomenon of valve impacts.

D. PISTON CLEARANCE EFFECT

Increased piston clearance increased the vibration levels in the mid frequency range while the engine was being fired, Figures III and IV.*

This increase occured during combustion which shows that the increased pressure increases the magnitude of the piston slap. This effect is greater, the greater the clearance. The increase in level for the 0.008 inch piston clearance above 6300 cycles was due to slightly greater valve clearance for these runs.

The radiated noise levels also increased as the piston clearance was made larger, Figures V and VI. In these cases the increase was evident over a greater range in frequency. For the firing runs the engine was kept as cool as possible to maintain the measured piston clearances. Therefore

---

*) The figures giving vibration level are all for position # 1 because lines from the lube oil pump showed up at position # 2.

the engine was not run at its most efficient combustion condition. Figure XI shows the increase in piston slap vibration magnitude, following 0 degrees crank angle, as the clearance was increased from .002 to .011 inches.

Figures VII and VIII show the same sort of increase in vibration level with increased clearance when the engine is motored instead of fired. It can be seen that the levels at higher frequency have been greatly reduced as the valve linkages were disconnected. For these particular runs there was no flow of air through the engine because the valves were always closed. Therefore these runs do not exactly simulate compressor conditions because the cylinder pressures were not as high as when the engine was motored with the valves operating.

At 800 RPM the radiated noise level showed very little change with piston clearance, Figure IX. This was because the impacts were not significant at such low speed. In Figure X when speed was increased to 1400 RPM, once again radiated noise increased with piston clearance.

E. DEPENDENCY ON SPEED

Figures XII, XIII, XIV, and XV show that noise and vibration levels are even more dependent on speed than on piston clearance. The increase in levels with speed showed up over almost the entire frequency band studied, while piston clearance effected only the mid frequencies. Figure XVI when compared with the bottom half of Figure XI shows that the peak vibration levels increase as the engine speed is increased from 800 to 1000 RPM. In these Figures the combustion can be seen at 0 degrees crank angle with the most severe piston slap following it. Then comes the opening of the exhaust valve and a piston slap. At 360 degrees the closing of the exhaust valve can be seen. There is another slap and then the intake valve closes at about 580 degrees.

F. COMBUSTION AND VALVE NOISE

Figures XVII and XVIII show that the mid frequency vibration levels are about six db higher when the engine is fired instead of motored. At high frequencies the levels are the same, as combustion has no effect on the valve noise. In Figures XIX and XX the radiated noise levels are about ten db higher at 800 cycles when the engine is fired. The levels when motored with and without rocker arms and tappets lifted are nearly the same out to 1000 cycles. Then at the higher frequencies the levels drop for the case of disconnected valve linkages.

Figure XXI shows the timing and magnitudes of the impacts for the three cases just discussed. In the picture for rocker arms and tappets lifted the peaks appear higher because the sensitivity was greater by a factor of ten.

Figure XXII shows the impacts experienced by the piston. It shows the slap following 0, 180, 360, and 540 degrees plus two in between.

A comparison of the overall radiated noise level for this engine was made with the correlation by Zinchenko of the Russian diesel engines he studied. The overall level compared very favorably using the empirical formula $L = 88 + 10 \log q + 28 \log ND$, where L is the sound pressure level (re 0.0002 microbar) at 1 meter, q is the number of cylinders, N is revolutions per second, and D is the cylinder diameter in meters.

V. CONCLUSIONS

The experimental study of a single-cylinder CFR engine showed that while piston slap impacts are of smaller magnitude than calculated, they nevertheless dominate a significant part of the spectrum. This conclusion is based on the observation that both for the motored and fired engine, at a given speed, the sound and vibration levels in certain frequency bands increased with increased piston clearance. In this particular engine, combustion and valve impacts were also important noise sources.

From the present analytical and experimental study it may also be concluded that:

1. Negative offset decreases the maximum transverse force acting on the piston and thus decreases piston slap.

2. Any bearing slap would be of lower magnitude than piston slap.

3. The piston rings probably provide considerable retarding force to the transverse motion of the piston reducing the effect of piston slap.

4. Noise and vibration levels of an engine increase rapidly with speed.

5. Valve impact noise completely dominates the vibration levels at the highest audio frequencies. However, the valves do not have such a large effect on the radiated noise levels.

6. Combustion increases the mid frequency noise and vibration levels by 6 to 10 db above when the engine is motored. This is because the increased pressures during combustion substantially increase the magnitude of piston slap. This effect is greater, the greater the piston clearance.

7. The empirical formula $L = 88 + 10 \log q + 28 \log ND$ gives a good approximation of the radiated noise level in db at one meter.

VI. RECOMMENDATIONS

1. Reciprocating machines should be designed with a negative offset to reduce piston slap.

2. Reciprocating machines should be run with as small piston clearances as is possible.

3. Machines of this type should be run at as slow a speed as is possible to do the job.

4. Overhead valves and linkages should be covered to reduce radiated noise.

5. Reciprocating machines that have ports instead of valves should be used when possible.

6. The empirical formula $L = 88 + 10 \log q + 28 \log ND$ should be used to select the diesel engine that has the lowest radiated noise when this is important.

7. A correlation of numerous diesel engine vibration data should be made in order to obtain an empirical formula to predict vibration levels.

APPENDIX

APPENDIX A

ANALYSIS OF IMPACTS

1. PISTON SLAP WITH OFFSET

To aid in the analysis, Figure A-I is provided to define the geometry and sign convention. The figure also contains a "free body" diagram showing the forces.

If the motion of the piston in the y-direction is very small, its x-direction displacement is given by

$$X_P = R \cos \Theta + L \cos \varphi \,. \qquad (A - 1)$$

The displacement of C, the connecting rod center of gravity, is given by

$$\begin{aligned} X_C &= R \cos \Theta + L_R \cos \varphi \\ Y_C &= L_P \sin \varphi + \delta_2 \,. \end{aligned} \qquad (A - 2)$$

From the geometry, the relation between φ and the crank angle Θ is given by

$$\delta_1 + R \sin \Theta = \delta_2 + L \sin \varphi$$

or

$$\sin \varphi = \gamma \sin \Theta + \delta \,, \qquad (A - 3)$$

where $\gamma = \frac{R}{L}$

and $\delta = \frac{\delta_1 - \delta_2}{L}$.

Substituting Eq. (A-3) and the small angle approximation

$$\cos \varphi \approx 1 - \frac{\gamma^2 \sin^2 \Theta}{2} - \delta\gamma \sin \Theta$$

since $\gamma^2 \ll 1$

and $\delta \ll \gamma$

into Eqs.(A-1) and (A-2), it is found

$$X_P = R\cos\Theta - L\,\delta\,\gamma\sin\Theta + L - L\,\frac{\gamma^2}{2}\sin^2\Theta$$

$$X_C = R\cos\Theta - L_R\,\delta\,\gamma\sin\Theta + L_R - L_R\,\frac{\gamma^2}{2}\sin^2\Theta$$

$$Y_C = L_P\,\gamma\sin\Theta + L_P\,\delta + \delta_2 \ .$$

Taking the second derivatives with respect to time, the accelerations are found to be

$$\begin{aligned}
\ddot{X}_P &= -R\omega^2(\cos\Theta - \delta\sin\Theta + \gamma\cos 2\Theta) \\
\ddot{X}_C &= -\omega^2(R\cos\Theta - L_R\,\delta\sin\Theta + L_R\,\gamma^2\cos 2\Theta) \\
\ddot{Y}_C &= -\omega^2 L_P\,\gamma\sin\Theta .
\end{aligned} \qquad (A-4)$$

under the usual assumption that $\dot{\omega} = 0$.

From Figure A-I it is seen that setting the x-direction forces on the piston equal to zero gives

$$F_{CP}^{x} = -F_G - F_P^{x\ddot{i}} \qquad (A-5)$$

where F_G is the force the gas pressure exerts on the piston.

Taking moments about point zero gives

$$\begin{aligned}
&F_C^{y\ddot{i}}\,L_R\cos\varphi + F_C^{x\ddot{i}}\,L_R\sin\varphi - F_{CP}^{y}\,L\cos\varphi - \\
&\quad F_{CP}^{x}\,L\sin\varphi + T_{CP} - T_{RC} = M_C(r^2 + L_R^2)\,\ddot{\varphi}
\end{aligned} \qquad (A-6)$$

where r denotes the radius of gyration of the connecting rod about an axis through its center of gravity.

Substituting Eq.(A-5) into Eq.(A-6) and solving for F_{CP}^{y}, the transverse force on the piston when it does not touch the cylinder wall, one finds

$$\begin{aligned}
F_{CP}^{y} = {} & F_C^{y\ddot{i}}\,\frac{L_R}{L} + F_C^{x\ddot{i}}\,\frac{L_R}{L}\tan\varphi - [-F_G - F_P^{x\ddot{i}}]\tan\varphi + \\
& \frac{T_{CP} - T_{RC}}{L\cos\varphi} - \frac{M_C(r^2 + L_R^2)\,\ddot{\varphi}}{L\cos\varphi} \ .
\end{aligned} \qquad (A-7)$$

Now by substituting in the expressions for the D'Alembert Forces and the small angle approximations

$$\tan\varphi \approx (\gamma \sin\Theta + \delta)\left(1 + \frac{\gamma^2 \sin^2\Theta}{2} + \delta\gamma \sin\Theta\right)$$

and

$$\ddot{\varphi} \approx -\gamma\omega^2 \sin\Theta \cos\varphi \,(1 - \gamma^2 \cos 2\Theta + 2\delta\gamma \sin\Theta),$$

Eq.(A-7) can be expressed in the form:

$$\frac{F^{y}_{CP}}{M_P R\omega^2} = \Phi_G + \Phi_P + \Phi_T + \Phi_C \qquad (A-8)$$

where the right-hand terms denote the contributions of gas force, piston inertia, friction torques, and connecting rod inertia, respectively, and:

$$\Phi_G = \Psi_G(\Theta)\tan\varphi \approx \Psi_G(\Theta)(\gamma\sin\Theta + \delta)\left(1 + \frac{\gamma^2\sin^2\Theta}{2} + \delta\gamma\sin\Theta\right)$$

$$\Phi_P = -(\cos\Theta - \delta\sin\Theta + \gamma\cos 2\Theta)\tan\varphi$$

$$\approx -(\cos\Theta - \delta\sin\Theta + \gamma\cos 2\Theta)(\gamma\sin\Theta + \delta)\left(1 + \frac{\gamma^2\sin^2\Theta}{2} + \delta\gamma\sin\Theta\right) \qquad (A-9)$$

$$\Phi_T = \frac{T_{CP} - T_{RC}}{M_P R\omega^2 L\cos\varphi} \approx \frac{T_{CP} - T_{RC}}{M_P R\omega^2 L\left(1 - \frac{\gamma^2\sin^2\Theta}{2} - \delta\gamma\sin\Theta\right)}$$

$$\Phi_C = -\mu\ell\left[(1-\ell)\sin\Theta + \left(\cos\Theta - \frac{\delta\ell}{\gamma}\sin\Theta + \ell\gamma\cos 2\Theta\right)\tan\varphi + \frac{(\rho^2 + \ell^2)\ddot{\varphi}}{\gamma\ell\omega^2\cos\varphi}\right]$$

$$\approx -\mu\ell\left[(1-\ell)\sin\Theta + \left(\cos\Theta - \frac{\delta\ell}{\gamma}\sin\Theta + \ell\gamma\cos 2\Theta\right)(\gamma\sin\Theta + \delta)\left(1 + \frac{\gamma^2\sin^2\Theta}{2} + \delta\gamma\sin\Theta\right) - \frac{1}{\ell}(\rho^2 + \ell^2)\sin\Theta\,(1 - \gamma^2\cos 2\Theta + 2\delta\gamma\sin\Theta)\right]$$

where $\Psi_G(\Theta) = \dfrac{F_G(\Theta)}{M_P R\omega^2}$

$$\mu = \frac{M_C}{M_P}$$

$$\ell = \frac{L_R}{L}$$

$$\rho = \frac{r}{L} \quad .$$

Noticing that Φ_T is the ratio of the net friction torque to the torque the centrifugal force $M_P R\omega^2$ acting with a lever arm L would exert, it is seen that Φ_T is small for all practical cases and it will therefore be neglected. Also, since $\gamma^2 \ll 1$ and $\delta\gamma \ll 1$, Eqs.(A-9) can be written in the reduced form:

$$\Phi_G(\Theta) \approx \Psi_G(\Theta)\,(\gamma \sin\Theta + \delta)$$

$$\Phi_P(\Theta) \approx -(\cos\Theta - \delta \sin\Theta + \gamma \cos 2\Theta)\,(\gamma \sin\Theta + \delta) \qquad \text{(A - 10)}$$

$$\Phi_C(\Theta) \approx -\mu\ell\left[(\cos\Theta - \frac{\delta\ell}{\gamma}\sin\Theta + \ell\gamma\cos 2\Theta)\,(\gamma\sin\Theta + \delta) + (1 - 2\ell - \frac{\rho^2}{\ell})\sin\Theta\right] \quad .$$

Eqs.(A-10) thus give the ratio of the transverse force on the piston to the centrifugal force $M_P R\omega^2$ as a function of crank angle since

$$\frac{F_{CP}^{y}(\Theta)}{M_P R\omega^2} \approx \Phi_G(\Theta) + \Phi_P(\Theta) + \Phi_C(\Theta) \quad . \qquad \text{(A - 11)}$$

The values for which the right-hand side of Eq.(A-11) become zero can be found by means of a graphical solution.

Now the velocity at impact can be determined. Since the clearance between the piston and cylinder wall is small, the piston will transverse

the distance while the crank angle changes only a few degrees. Thus the transverse force at the time of impact can be approximated by

$$\frac{F^{y}_{CP}(\Theta_o + \Delta\Theta)}{M_P R\omega^2} \approx \frac{\Delta\Theta \, d\left[F^{y}_{CP}(\Theta_o)\right]}{M_P R\omega^2 \, d\Theta} \qquad (A - 12)$$

where $\Delta\Theta$ is the small angle the crank travels from Θ_o, the crank angle at which the transverse force vanishes.

From Eqs.(A-10) and (A-12), one can obtain

$$\frac{1}{M_P R\omega^2} \frac{d\left[F^{y}_{CP}(\Theta_o)\right]}{d\Theta} = K(\Theta_o) \approx \Phi'_G(\Theta_o) + \Phi'_P(\Theta_o) + \Phi'_C(\Theta_o) \qquad (A - 13)$$

where $\Phi'_G(\Theta_o) \approx \frac{d\Psi_G(\Theta_o)}{d\Theta}(\gamma S + \delta) + \Psi_G(\Theta_o)\gamma C$

$$\Phi'_P \approx (S + \delta C + 4\gamma SC)(\gamma S + \delta) - (C - \delta S + \gamma - 2\gamma S^2)\gamma C \qquad (A - 14)$$

$$\Phi'_C \approx \mu\ell\left[(S + \frac{\delta\ell C}{\gamma} + 4\ell\gamma SC)(\gamma S + \delta) - (C - \frac{\delta\ell}{\gamma} S + \ell\gamma - 2\ell\gamma S^2)\gamma C - (1 - 2\ell - \frac{\rho^2}{\ell})C\right]$$

and $S = \sin\Theta_o$

$C = \cos\Theta_o$.

Then using Eq.(A-12), the transverse motion of the piston may be written as

$$F^{y}_{CP}(\Theta_o + \Delta\Theta) \approx \Delta\Theta \, K(\Theta_o) \, M_P R\omega^2 \approx M_P \ddot{y} = M_P \omega^2 \frac{d^2 y}{d\Delta\Theta^2} . \qquad (A - 15)$$

Integrating this expression twice gives:

$$\Delta\Theta = \left[\frac{6}{K(\Theta_o)} \left(\frac{d}{R}\right)\right]^{1/3} \qquad (A - 16)$$

where d is the clearance distance.

This expression assumes that there are no retarding forces such as friction due to oil or any forces on the piston rings. It also neglects the possibility of the piston canting about the wrist pin. Now the velocity at impact can be obtained from the relation $V_o = \dot{y}\,(\Theta_o + \Delta\Theta)$ which gives

$$V_o = \frac{R\omega}{2}(\Delta\Theta)^2\ K(\Theta_o) = R\omega\left[\frac{9}{2}\left(\frac{d}{R}\right)^2 K(\Theta_o)\right]^{1/3} \qquad (A - 17)$$

2. BEARING SLAP IMPACTS

The analysis for the connecting rod bearing slap at 0 begins with the same general analysis as in Section A except there is no offset. Therefore $\delta = 0$ in all the equations.

Eqs.(A-4) become

$$\ddot{X}_P = -R\omega^2(\cos\Theta + \gamma\cos 2\Theta)$$

$$\ddot{X}_C = -R\omega^2(\cos\Theta + \gamma\ell\cos 2\Theta) \qquad (A - 18)$$

$$\ddot{Y}_C = -\omega^2 L_P \gamma \sin\Theta \quad .$$

The x-direction forces on the piston are still given by Eq.(A-5).

The x-direction forces on the connecting rod when set equal to zero give

$$F_{RC}^{x} = -F_{CP}^{x} + F_C^{x\ddot{\imath}} \qquad (A - 19)$$

Substituting Eq.(A-5) and the expression for the D'Alembert Forces into Eq.(A-19), one finds for the x-direction reaction at 0

$$F_{RC}^{x} = F_G - M_P R\omega^2(\cos\Theta + \gamma\cos 2\Theta) - M_C R\omega^2(\cos\Theta + \gamma\ell\cos 2\Theta). \qquad (A - 20)$$

This may be expressed as

$$\frac{F^{x}_{RC}(\Theta)}{M_P R\omega^2} = \Phi_{G_1}(\Theta) + \Phi_{P_1}(\Theta) + \Phi_{C_1}(\Theta) \qquad (A-21)$$

where

$$\Phi_{G_1}(\Theta) = \Psi_G(\Theta)$$

$$\Phi_{P_1}(\Theta) = -(\cos\Theta + \gamma\cos 2\Theta) \qquad (A-22)$$

$$\Phi_{C_1}(\Theta) = -\mu(\cos\Theta + \gamma\ell\cos 2\Theta) \quad .$$

Setting the y-direction forces on the connecting rod equal to zero one finds:

$$F^{y}_{CP} = -F^{y}_{RC} + F^{y\ddot{\imath}}_{C} \quad . \qquad (A-23)$$

Then taking moments about C, but neglecting the friction torques gives

$$F^{y}_{RC} L_R \cos\varphi + F^{x}_{RC} L_R \sin\varphi - F^{y}_{CP} L_P \cos\varphi - F^{x}_{CP} L_P \sin\varphi = M_C r^2 \ddot{\varphi} \quad . \qquad (A-24)$$

Substituting Eqs.(A-5), (A-19), and (A-23) into Eq.(A-24) and solving for F^{y}_{RC}, the y-direction reaction at 0, one finds

$$F^{y}_{RC} = -F_G \tan\varphi - F^{x\ddot{\imath}}_{P} \tan\varphi - F^{x\ddot{\imath}}_{C} \ell \tan\varphi + F^{y\ddot{\imath}}_{C}(1-\ell) + \frac{M_C r^2 \ddot{\varphi}}{L\cos\varphi} \quad . \qquad (A-25)$$

By substituting in the expressions for the D'Alembert Forces and the small angle approximations for $\tan\varphi$ and $\ddot{\varphi}$ with $\delta = 0$, Eq.(A-25) can be expressed in the form:

$$\frac{F^{y}_{RC}(\Theta)}{M_P R\omega^2} = \Phi_{G_2}(\Theta) + \Phi_{P_2}(\Theta) + \Phi_{C_2}(\Theta) \qquad \text{(A - 26)}$$

where

$$\Phi_{G_2}(\Theta) \approx - \Psi_G(\Theta)\, \gamma \sin\Theta \left(1 + \frac{\gamma^2 \sin^2\Theta}{2}\right)$$

$$\Phi_{P_2}(\Theta) \approx (\cos\Theta + \gamma \cos 2\Theta)\, \gamma \sin\Theta \left(1 + \frac{\gamma^2 \sin^2\Theta}{2}\right) \qquad \text{(A - 27)}$$

$$\Phi_{C_2}(\Theta) \approx \mu \sin\Theta \left[- (1-\ell)^2 + \gamma\ell (\cos\Theta + \gamma\ell \cos 2\Theta) \left(1 + \frac{\gamma^2 \sin^2\Theta}{2}\right)\right.$$

$$\left. - \rho^2 (1 - \gamma^2 \cos 2\Theta) \right] .$$

Since $\frac{\gamma^2}{2} \ll 1$, Eqs. (A-26) can be written in the reduced form

$$\Phi_{G_2}(\Theta) \approx - \Psi_G(\Theta)\, \gamma \sin\Theta$$

$$\Phi_{P_2}(\Theta) \approx (\cos\Theta + \gamma \cos 2\Theta)\, \gamma \sin\Theta \qquad \text{(A - 28)}$$

$$\Phi_{C_2}(\Theta) \approx \mu \left[\frac{-(1-\ell)^2 - \rho^2}{\gamma} + \ell \cos\Theta + \gamma (\ell^2 + \rho^2) \cos 2\Theta \right] \gamma \sin\Theta$$

Eqs. (A-22) and (A-28), the x and y components of the reaction vector at point 0, can now be plotted and the vector determined for any crank angle.

The crankshaft main bearings are located at point A in Figure A-I.

The motion of the crankshaft center of gravity is given by

$$X_B = R_B \cos\Theta$$
$$Y_B = R_B \sin\Theta \quad . \qquad \text{(A - 29)}$$

Taking the second derivatives with respect to time, the accelerations are found to be

$$\ddot{X}_B = - R_B \omega^2 \cos\Theta$$
$$\ddot{Y}_B = - R_B \omega^2 \sin\Theta \quad . \qquad \text{(A - 30)}$$

Setting the x-direction forces acting on the crankshaft equal to zero gives

$$F_A^x = F_{RC}^x + F_B^{x\lambda} \quad . \qquad (A - 31)$$

Substituting the D'Alembert Force into Eq.(A-31) and making the expression dimensionless gives

$$\frac{F_A^x}{M_P R\omega^2} = \frac{F_{RC}^x}{M_P R\omega^2} - \nu\lambda \cos\Theta \qquad (A - 32)$$

where

$$\nu = \frac{M_R}{M_P}$$

$$\lambda = \frac{R_B}{R} \quad .$$

Now Eq.(A-32) can be expressed as

$$\frac{F_A^x}{M_P R\omega^2} = \Phi_{G_1}(\Theta) + \Phi_{P_1}(\Theta) + \Phi_{C_1}(\Theta) + \Phi_{R_1}(\Theta) \qquad (A - 33)$$

where the first three terms on the right hand side of the equation are Eqs.(A-22) and $\Phi_{R_1}(\Theta) = -\nu\lambda \cos\Theta$. (A - 34)

In exactly the same manner it can be shown that

$$\frac{F_A^y}{M_P R\omega^2} = \Phi_{G_2}(\Theta) + \Phi_{P_2}(\Theta) + \Phi_{C_2}(\Theta) + \Phi_{R_2}(\Theta) \qquad (A - 35)$$

where the first three terms on the right hand side of the equation are Eqs.(A-28) and $\Phi_{R_2}(\Theta) = -\nu\lambda \sin\Theta$. (A - 36)

Using Eqs.(A-33) and (A-35), the reaction vector at point A, the crankshaft main bearings, can be determined. Eq.(A-17) which gives the impact velocity could also be used for this case. $K_1(\Theta_0)$ for the x-direction and $K_2(\Theta_0)$ for the y-direction could be obtained by differentiating

with respect to Θ, Eqs.(A-33) and (A-36) respectively. Θ_o can be determined from a graphical solution of these two equations.

3. VALVE IMPACTS

The engine studied had overhead valves. The cam and tappet arrangement was as shown in Figure A-II. The cam consisted of a circular arc and two straight line segments tangent to the arc. The tappets had a circular base that was flat.

The valve impacts occur as the valve seats on the engine head. This happens just before the straight segment of the cam becomes tangent to the tappet base. Figure A-III shows the geometry for this happening. From the Figure it is seen that

$$y = \frac{a}{\cos \Theta} + b \tan \Theta \qquad \text{(A - 37)}$$

$$\text{and} \quad \dot{y} = \frac{\omega a \sin \Theta}{\cos^2 \Theta} + \omega b \sec^2 \Theta$$

$$\text{or} \quad \dot{y} = \frac{\omega}{\cos^2 \Theta} (a \sin \Theta + b) \ . \qquad \text{(A - 38)}$$

The valve has a velocity equal in magnitude and opposite in direction to the tappet, as a pushrod goes directly to a rocker arm which is pivoted around its midpoint.

The angle Θ, at which the valve seats, is determined by the clearance d, which is set between the rocker arm and the valve stem. The valve seats when

$$y = a + d \ . \qquad \text{(A - 39)}$$

Thus from Eq.(A-37) one gets

$$a + d = \frac{a}{\cos \Theta} + b \tan \Theta$$

$$\text{or} \qquad (a + d) \cos \Theta = a + b \sin \Theta. \qquad \text{(A - 40)}$$

Θ can be obtained from Eq.(A-40) and then Eq.(A-38) can be used to solve for the valve impact velocity.

FIGURE A-I

Geometry and Forces for Piston Offset Analysis

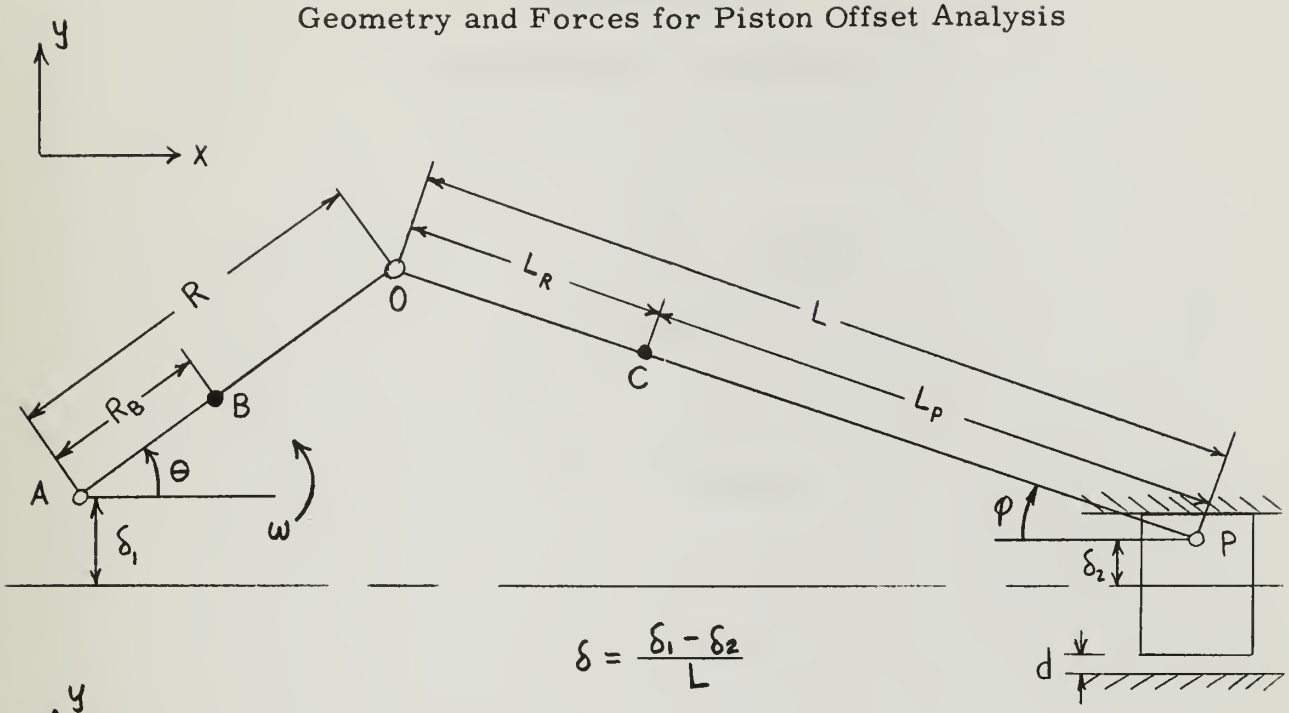

$$\delta = \frac{\delta_1 - \delta_2}{L}$$

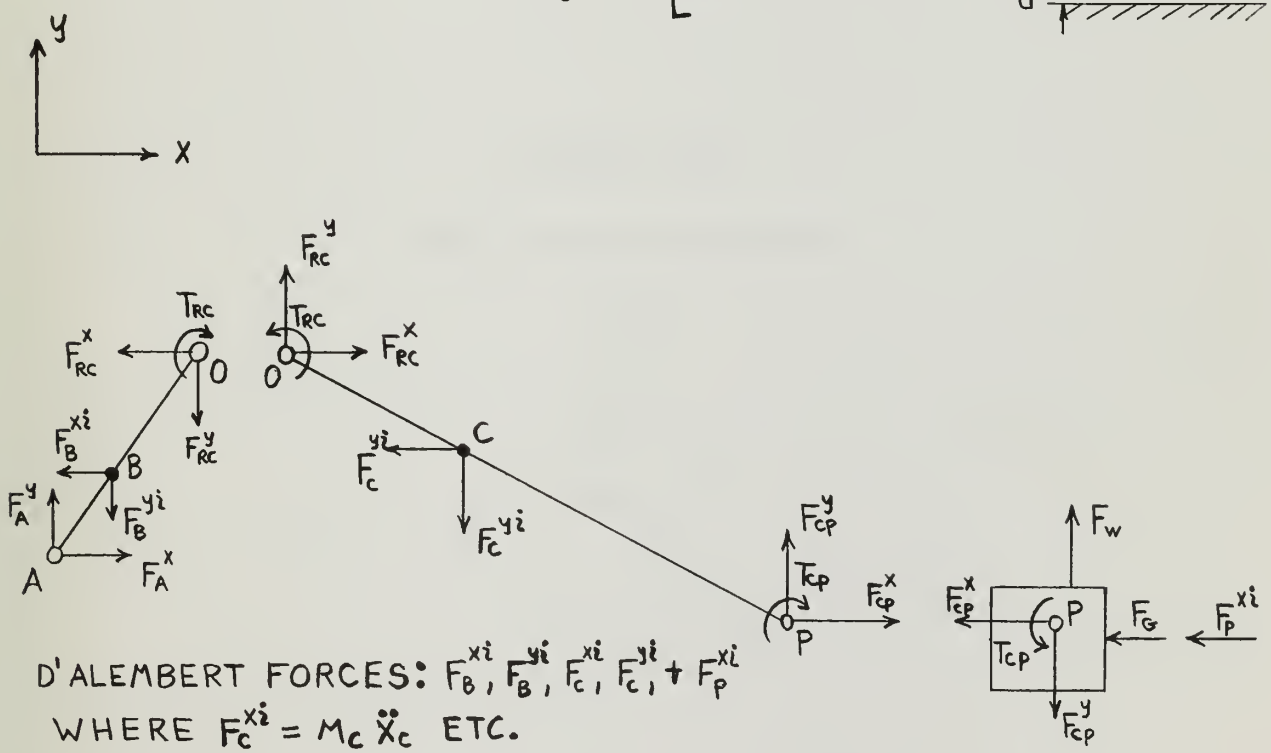

D'ALEMBERT FORCES: $F_B^{xi}, F_B^{yi}, F_C^{xi}, F_C^{yi} + F_P^{xi}$

WHERE $F_C^{xi} = M_C \ddot{X}_C$ ETC.

FIGURE A-II

Cam and Tappet Arrangement

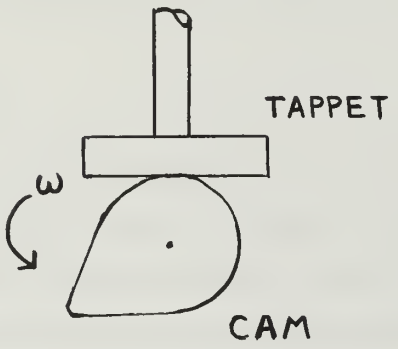

FIGURE A-III

Cam and Tappet Geometry

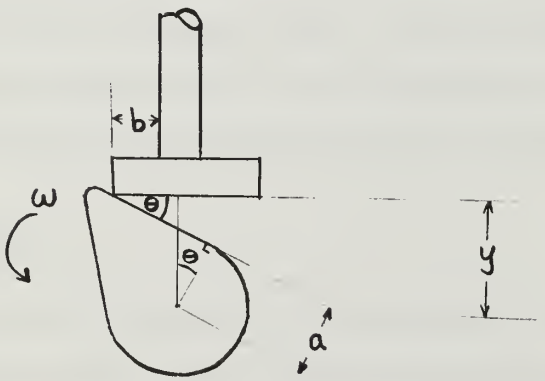

APPENDIX B

DETAILS OF PROCEDURE

1. INSTRUMENTATION

The instrumentation for the experiments consisted of a third active band frequency analyser and an oscilloscope. The analyser was used to obtain sound pressure level and acceleration spectra for the diesel by using both a microphone and an acceleration pickup. The signals were first run through a sound level meter used as an amplifier, Figure B-I. The oscilloscope was used to time the various engine impacts in relation to top dead center, i.e. crank angle, as well as to record the peak magnitudes. In order to mark TDC for a reference on the oscilloscope a proximity pickup was installed right above the flywheel which had a protrusion at TDC. Thus each time the engine reached TDC a voltage would appear on the trace of the oscilloscope. Since this was a four stroke engine, TDC was reached twice each complete engine cycle.

During the runs to record radiated noise, the microphone was placed one meter away from the cylinder head. The vibration data were obtained with the acceleration pickup at two locations shown in Figure B-II.

2. PRELIMINARY STEPS

Before any data could be obtained it was necessary to quiet certain engine parts. There was a noisy check valve in the intake piping, and the crankcase vent had to be quieted as well as the breaker points that were there for spark ignition use of the engine. Some of the higher peaks showing on the oscilloscope were identified by eliminating them and then letting them reappear. For the valves this was accomplished by using a feeler gauge to keep them from seating. The fuel injection noise was

identified by disconnecting and reconnecting the coupling to the engine.

Cylinder pressure plots versus crankangle were obtained by using a point-by-point indicator. Indicator card readings were taken at several speeds from 800 to 1400 RPM both when the engine was being fired and when it was motored. Also, before any runs were made the piston, connecting rod, valves, and valve linkages were weighed and their measurements recorded.

3. DATA RUNS CONDUCTED

Three distinct types of runs were conducted. The first type were runs to simulate conditions of a compressor. For these the valve rocker arms and tappets were lifted, and the fuel injector coupling was disconnected. Although there was cooling water to the jacket, the circulating pump was not running in order to reduce the background noise level. These were motoring runs. Since several different piston sizes were to be used and there was a scarcity of the special pistons used to convert the engine to diesel firing, it was decided to use the standard smaller spark ignition pistons for this set of motoring runs.

The second type of runs were diesel firing runs with all parts of the engine running including the cooling water circulating pump. For these firing runs the fuel injection timing was set at eight degrees before TDC.

The third type of runs were motoring runs made under the same conditions as the firing runs only without the fuel being injected. This was to examine what effect the combustion had on the noise and vibration levels. These same runs were then repeated with the valve rocker arms and tappets lifted to eliminate the valve noise. Runs were also made with the piston and connecting rod removed from the engine so that all piston slap would be eliminated. A summary of all runs conducted is contained in Table B-I.

TABLE B-I

SUMMARY OF DATA RUNS CONDUCTED

Type	RPM	Piston Clearance	Piston Type	Instrumentation	Rocker Arms and Tappets Lifted
Motored	800, 1000, 1250, 1400	0.005	S	Acc. Posit. #1	Yes
Motored	800, 1000, 1250, 1400	0.005	S	Acc. Posit. #2	Yes
Motored	800, 1400	0.005	S	Micro.	Yes
Motored	800, 1000, 1250, 1400	0.008	S	Acc. Posit. #1	Yes
Motored	1250	0.008	S	Acc. Posit. #2	Yes
Motored	800, 1250, 1400	0.008	S	Micro.	Yes
Motored	800, 1000, 1250, 1400	0.011	S	Acc. Posit. #1	Yes
Motored	1400	0.011	S	Acc. Posit. #2	Yes
Motored	800, 1250, 1400	0.011	S	Micro.	Yes
Fired	800, 1000, 1250, 1400	0.002	D	Acc. Posit. #1	No
Fired	800, 1000, 1250, 1400	0.002	D	Micro.	No
Motored	800, 1000, 1250, 1400	0.002	D	Acc. Posit. #1	No
Motored	800, 1000, 1300, 1400	0.002	D	Micro.	No

TABLE B-I (CONT'D)

Motored	800, 1000, 1300, 1400	0.002	D	Acc. Posit. #1	Yes
Motored	800, 1000, 1300, 1400	0.002	D	Micro.	Yes
Fired	800, 1000, 1250, 1400	0.008	D	Acc. Posit. #1	No
Fired	800, 1000, 1300, 1400	0.008	D	Micro.	No
Motored	800, 1000, 1250, 1400	0.008	D	Acc. Posit. #1	No
Motored	800, 1000, 1300, 1400	0.008	D	Micro.	No
Motored	800, 1000, 1300, 1400	0.008	D	Acc. Posit. #1	Yes
Motored	800, 1000, 1300, 1400	0.008	D	Micro.	Yes
Fired	800, 1000, 1400	0.011	D	Acc. Posit. #1	No
Fired	800, 1000, 1400	0.011	D	Micro.	No
Motored	800, 1000, 1400	0.011	D	Acc. Posit. #1	No
Motored	800, 1000, 1400	0.011	D	Micro.	No
Motored	800, 1000, 1400	0.011	D	Acc. Posit. #1	Yes
Motored	800, 1000, 1400	0.011	D	Micro.	Yes

TABLE B-I (CONT'D)

Motored	800, 1000, 1250, 1400	Removed	-	Acc. Posit. #1	Yes
Motored	800, 1000, 1250, 1400	Removed	-	Acc. Posit. #1	No

In simulating the impacts the ball bearing was dropped on both the outside of the jacket and inside on the liner, and very little difference was noticed. To make the inside drops it was necessary to support the head of the engine on a nonstiff frame. The jacket was filled with water and then plugged in order to give the same transfer characteristics as the operating engine.

FIGURE B-I

Schematic Drawing of Instrumentation

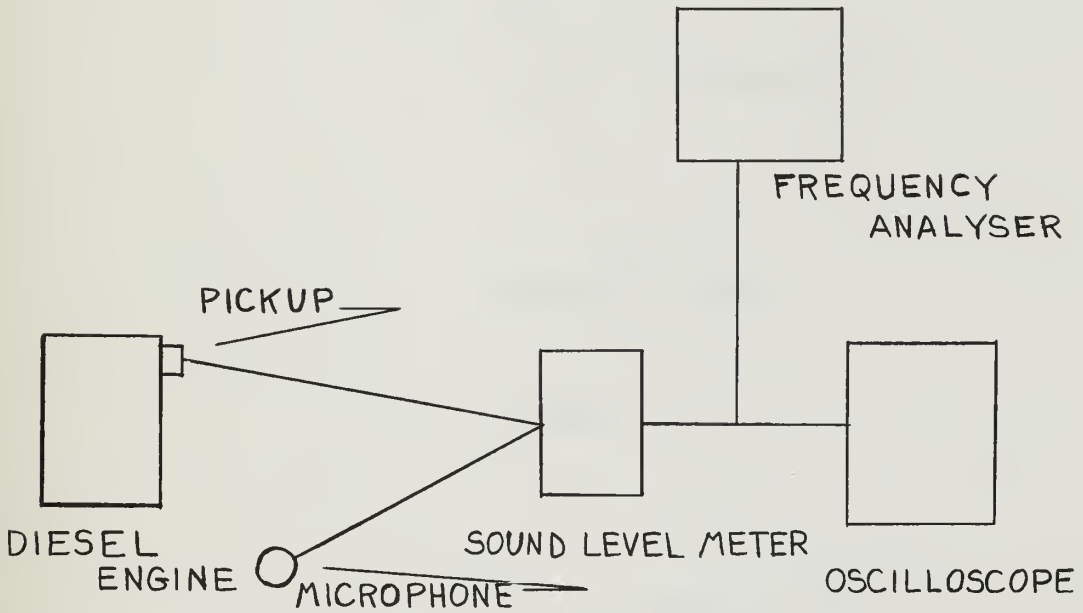

FIGURE B-II

Location of Microphone and Acceleration Pickup

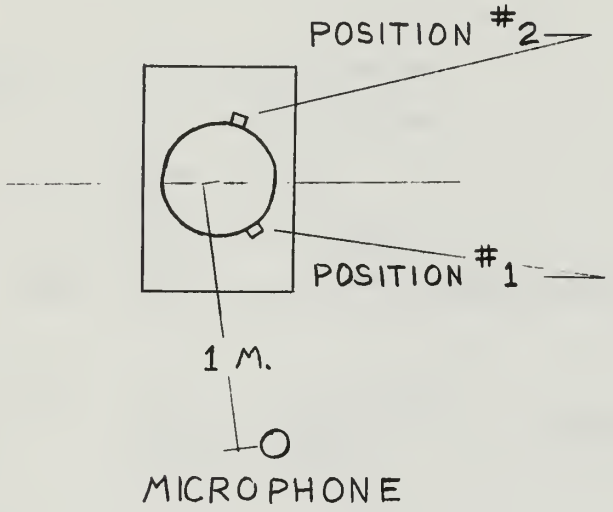

PLAN

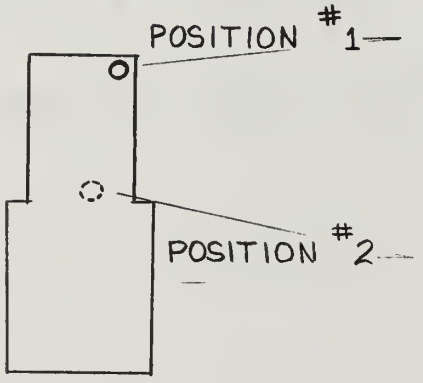

ELEVATION

APPENDIX C

SAMPLE CALCULATIONS

For the piston, where $d = 0.011$ inches

$R = 2.25$ inches

RPM = 1000

$M_P = .149$ slugs

and $K(o) = 1.96$, determined from Eq.(A-13),

$$\Delta\Theta = \left[\frac{6}{K(o)}\left(\frac{d}{R}\right)\right]^{1/3} = \left[\frac{6}{1.96}\left(\frac{.011}{2.25}\right)\right]^{1/3} = .246 \text{ radians}$$

$\Delta\Theta = \underline{14.1 \text{ degrees.}}$

$$\omega = \frac{1000}{60}(2\pi) = 105 \text{ rad./sec.}$$

$$\text{K.E.} = \frac{1}{2} MV^2 = \frac{1}{2} M_P(R\omega)^2 \left[4.5 \left(\frac{d}{R}\right)^2 K(o)\right]^{2/3}$$

$$\text{K.E.} = \frac{1}{2}(.149)\left(\frac{2.25}{12}\right)^2 (105)^2 \left[4.5\left(\frac{.011}{2.25}\right)^2 1.96\right]^{2/3}$$

$$= (28.9)(.0033)$$

K.E. = $\underline{.095 \text{ ft-lbs.}}$

For the valve, where $d = .010$ inches

$a = .657$ inches

$b = .610$ inches

RPM = 800

and $Mv = .00485$ slugs,

Eq.(A-40) shows that $\Theta \approx 0^{o}$.

$\omega = \frac{800}{2(60)}(2\pi) = 42$ rad./sec. as the camshaft speed is one half the engine speed.

$$K.E. = \frac{1}{2} MV^2 = \frac{1}{2} Mv \left[\frac{\omega (a \sin \Theta + b)}{\cos^2 \Theta \quad 12}\right]^2$$

$$K.E. = \frac{1}{2}(.00485) \left[\frac{42 (.610)}{12}\right]^2 = (.00242)(4.52)$$

K.E. = .011 ft-lbs.

APPENDIX D

BIBLIOGRAPHY

1. Austen, A. E. W., and Priede, T., "Origins of Diesel Engine Noise," SAE Paper 125T, National Diesel Engine Meeting, October 1959; also, Inst. of Mechanical Engineers Symposium on Engine Noise and Suppression, 1959; and,

2. Priede, T., "Noise of Internal Combustion Engines," Paper C-2, NPL Symposium on the Control of Noise, June 1961.

Papers deal with studies of diesel and spark-ignition automotive engines carried out at C. A. V. Ltd., Acton, England. Cylinder pressures and noise were measured for motored and fueled engines, with various injection characteristics and timing. Attempt was made to correlate observed noise spectra and cylinder pressure spectra. "Attenuation spectra" are derived from measured noise and cylinder pressure spectra. Similarity of noise spectra for motorized and fueled engines in spite of drastic changes in cylinder pressure spectrum is explained in terms of a "critical cylinder pressure level" below which engine mechanical noise dominates. Observed increase of noise with speed of 30 db/decade is explained in terms of the slope of the cylinder pressure spectrum. A 5 db increase in overall sound pressure level is obtained for each doubling of power (measured in terms of displacement volume) at constant speed (rpm). Observed sound power levels of all engines tested were between about 80 and 100 db. (These are considerably lower than levels generally obtained with marine diesels.) For automotive diesels overall sound pressure level at 3 feet is given by

$$\text{SPL (db re 0.0002 microbar, at 3 ft)} \approx$$

$$75 + 17 \log V \text{ (liters)} + 30 \log \frac{N \text{ (rpm)}}{1000}$$

where V denotes the total displacement and N the engine rotational speed. Peak octave-band sound pressure found at about 1 or 2 kc for engines operating between 1000 and 2000 rpm. Conclusion is drawn that for a given mechanical output power larger slower running engines are quieter, since speed increases produce greater noise level changes than displacement increases.

3. Biezeno, C.B. and Grammel, R., Engineering Dynamics, v. 4, (1954).

Book gives a complete analysis of the forces and torques acting on an internal combustion engine. Also discusses various ways to eliminate unbalance in an engine.

4. Bradbury, C.H., "The Measurement and Interpretation of Mechanical Noise with Special Reference to Oil Engines," The Institution of Mechanical Engineers, Proceedings, v. 1B, pp 1 - 8, (1952-53).

Paper discusses diesel engine noise and its causes. It recognizes piston-slap as a noise source and accordingly recommends that the skirts of the pistons be fitted with close tolerances. Data indicative of the occurrence of piston-slaps in a running diesel are included.

5. Craig, W.W., "Theoretical Relationship Between Combustion Pressure and Engine Vibration," Society of Automotive Engineers, Paper No. 647C, (Jan. 1963).

Paper follows ideas of Austen and Priede and extends development of relation between combustion pressure and engine vibration. Single CFR engine is studied, analysis based on lumped parameter model. He finds that at higher frequencies vibration intensities are proportional to rate of change of slope of pressure-time curve, at mid-frequencies vibration intensities are proportional to slope of pressure-time curve, at low frequencies vibration intensities are proportional to combustion pressure. Noise levels measured with four different compression ratios and five different spark timings differed by at most 11 db at 300 cps and 18 db at 1200 cps. Differences attributed to combustion energy differences, as derived from derivative of pressure-time curve.

6. Crane, P.H.G., "The Initiation of Diesel Cylinder Liner Vibrations by Piston Transverse Motion," Admiralty Research Laboratory Report R2/B10, (August 1959).

Develops expressions for transverse force between piston and cylinder liner and sets up nonlinear equation of motion for piston across cylinder clearance space. Studies impact velocity and energy for three large diesels by means of numerical calculations, including effects of connecting rod and piston ring inertia, piston ring friction, and axial offsets between piston center of gravity and wrist pin. Concludes that lateral piston impacts may be responsible for cavitation in cooling water surrounding cylinder liners, and thus for cavitation-induced cylinder liner damage.

7. Davies, A. J., "Injection Characteristics and Diesel Knock," Proceedings of the Institution of Mechanical Engineers, Automotive Division, pp 214-223, (1951-1952).

Paper discusses effects of combustion pressure changes on engine knock. Experiments are described and some graphical data on cylinder pressure and cylinder head vibrations are given.

8. Den Hartog, J. P., Mechanical Vibrations, 4th ed., pp 170-224, 229-232, (1956).

Book has an excellent chapter dealing with the dynamics and balancing of reciprocating machinery. Also has a section on flexural critical speeds for shafts.

9. Elford, W. E., "An Interim Report on the Causes of Waterside Attack on Diesel Engine Cylinder Liners," Admiralty Research Laboratory Report R. 1/B. 10.

Report gives evidence of high levels of high frequency vibration on cylinder liners due to piston slap.

10. Hobson, A., "Interim Report of Various Measurements of the Vibrations of Diesel Engines," Admiralty Research Laboratory Report R4/93.20/D, (May 1960).

Vibrations and cylinder pressures were measured on three diesels and a swash-plate engine. Vibration spectra of engines under full and light load, and motored with and without compression, were found to be very similar. In one engine a marked reduction in high frequency vibrations was obtained when engine was motored and camshaft was kept stationary. Typical vibration levels at the base of engines were 90 to 100 db re 10^{-6} cm/sec, in octave bands, between 100 and 2000 cps. Transfer impedance between cylinder and base of engine was measured by a "banger" method, in which gas was detonated in absence of mechanical motion. Comparison of measured transfer admittance with difference between vibration and cylinder pressure spectra led to conclusion that vibration levels at higher frequencies cannot be attributed to gas pressure or unbalance forces. Piston-slap is suggested as one possible source of vibration, but no analysis of this source is attempted.

11. Holowenko, A. R., Dynamics of Machinery, pp 124-134, 294-382, (1955).

Book has a chapter on the kinematics of cams. Also has several chapters on the dynamics and balancing of reciprocating machines.

12. Joyner, J.A., "Reduction of Cavitation Pitting of Diesel Engine Cylinder Liners," Society of Automotive Engineers, Transactions, v. 65, pp 337-348, (1957).

Paper reports measurements of cylinder liner vibrations undertaken to investigate the effect of piston side thrust on cylinder liner cavitation. Cylinder liner vibration amplitudes up to .006 inches were measured on thin wall liners, amplitudes as small as .001 inches were measured on thick wall liners for a 50 HP, 2000 rpm diesel engine. Excellent correlation between calculated piston side thrust and measured amplitudes of vibration was found. Paper recommends that piston clearances be reduced or cylinder liner walls be thickened to reduce liner vibration amplitudes.

13. Mercy, K.R., "The Diesel Engine Noise Problem," Paper presented at the Ship Noise Symposium, 1954, BuShips Report No. 371-N-22.

14. Mercy, K.R., "Analysis of the Basic Noise Sources in the Diesel Engine," American Society of Mechanical Engineers Paper No. 55-OGP-4 (March 1955).

15. Mat. Lab., New York Naval Shipyard, Project 5276, NS 713-212, Progress Report No. 11 (April 1959), Final Report, (4 April 1961).

Discusses noise and vibration measurements obtained on a GM 8-268A diesel engine with various parts of engine removed. Major noise sources in order of importance were found to be: blower, pistons and connecting-rods, exhaust valves, fuel injectors, combustion. Fully loaded engine found to be only 1 db noisier than engine under no load. A 10 db noise increase was observed when speed was changed from 600 to 1200 rpm. Spectra showed maximum noise to be below 500 cps.

16. Skorecki, J., "Vibration and Noise of Diesel Engines," American Society of Mechanical Engineers, Paper No. 63-OGP-2 (2 August 1962).

Paper compares sound emitted by an engine with its vibratory acceleration. Cites combustion pressure and mechanical impact (piston slap, etc.) as the two main sources of vibrations. Comparison of power and motoring runs showed combustion pressures to be the major high-frequency noise source.

17. Starkman, F.S. and Sytz, W.E., "The Investigation and Characterization of Rumble and Thus," Society of Automotive Engineers, Transactions, v. 68, pp 93-100, (1960).

17. Paper attributes "rumble" (with sound spectrum between 400 and 2000 cps) to bending vibrations of the crankshaft induced by high rates of combustion pressure rise near top dead center. Fuel and other engine operating factors are taken to determine the magnitudes of the various harmonics of the vibrations.

18. Taylor, C.F. and Taylor, E.S., The Internal Combustion Engine, 2nd ed., (1961).

Book is a complete text on reciprocating engine performance and operating characteristics.

19. Ungar, E.E., Ross, D., and Alvarez, F.F., "Piston-Slap Noise in Reciprocating Machinery," Bolt Beranek and Newman, Inc. Report No. 1106, (January 1964, Revised 15 April 1964).

Report contains a thorough analysis of the dynamics of piston slap. Gives relative magnitudes, number, and occurrence of these slaps for different cylinder pressure curves. Has discussion of vibrations and radiated noise induced by these slaps and presents techniques for estimating the corresponding noise and vibratory power. Also discusses the correlation of Zinchenko's diesel noise data with various engine parameters.

20. Zinchenko, V.I., "Effect of Constructional Factors on the Noise of Ships' Engines," Vestnik Mashinostroyeniya No. 4, pp 13-17, (1956).

21. Zinchenko, V.I., Noise of Marine Diesel Engines, Sudpromgiz (1957).

(Book is digested in Bolt Beranek and Newman Technical Information Report No. 61, (July 1962).)

Summarizes noise data obtained on 60 engines. Develops piston-slap concept as explanation of "mechanical" noise of diesel engines. Discusses some measurements of cylinder wall vibrations that show pulses due to piston impacts.